Molecular Pharmacology Fast Forward. Published on September 16, 2011 as doi:10.1124/mol.111.074989

Elucidating the molecular basis of action of a classical drug:

Guanidine compounds as inhibitors of voltage-gated potassium channels

Jeet Kalia and Kenton J. Swartz

Porter Neuroscience Research Center,

Molecular Physiology and Biophysics Section,

National Institute of Neurological Disorders and Stroke,

National Institutes of Health

35 Convent Drive,

Bethesda, Maryland 20892, USA (J. K., K. J. S.)

Molecular Pharmacology Fast Forward. Published on September 16, 2011 as DOI: 10.1124/mol.111.074989
This article has not been copyedited and formatted. The final version may differ from this version.

Running Title: Mechanism of inhibition of Kv channels by guanidine compounds

Corresponding Authors: Jeet Kalia (kaliaj@ninds.nih.gov) and Kenton Swartz (swartzk@ninds.nih.gov), Porter Neuroscience Research Center, Molecular Physiology and Biophysics Section, National Institute of Neurological Disorders and Stroke, National Institutes of Health, 35 Convent Drive, Bethesda, Maryland 20892, USA. Telephone: (301) 435-5652; Fax: (301) 435-5666.

Number of text pages: 33

Number of tables: 0

Number of figures: 8

Number of references: 40

Number of words in Abstract: 165

Number of words in Introduction: 714

Number of words in Discussion: 1016

List of non-standard abbreviations:

1) Kv channels: Voltage-gated potassium channels

2) Gdn: Guanidine

3) MeGdn: Methylguanidine

4) DiMeGdn: Dimethylguanidine

5) 4-AP: 4-aminopyridine

6) TEA: Tetraethylammonium

7) TRPM8: Transient Receptor Potential cation channel, subfamily M, member 8

Molecular Pharmacology Fast Forward. Published on September 16, 2011 as DOI: 10.1124/mol.111.074989
This article has not been copyedited and formatted. The final version may differ from this version.

Abstract.

Guanidine and its alkyl analogs stimulate the neuromuscular junction presynaptically by inhibiting voltage-gated potassium (Kv) channels, leading to enhanced release of acetylcholine in the synaptic cleft. This stimulatory effect of guanidine underlies its use in the therapy for the neuromuscular diseases, myasthenic syndrome of Lambert-Eaton and botulism. The therapeutic use of guanidine is limited, however, due to side effects that accompany its administration. Therefore, the design of guanidine analogs with improved therapeutic indices is desirable. Progress towards this goal is hindered by the lack of knowledge of the mechanism by which these molecules inhibit Kv channels. Here we examine an array of possible mechanisms, including charge screening, disruption of the protein-lipid interfaces, direct interaction with the voltage sensors and pore-binding. Our results demonstrate that guanidines bind within the intracellular pore of the channel, and perturb a hydrophobic subunit interface to stabilize a closed state of the channel. This mechanism provides a foundation for the design of guanidine analogs for the therapeutic intervention of neuromuscular diseases.

Molecular Pharmacology Fast Forward. Published on September 16, 2011 as DOI: 10.1124/mol.111.074989
This article has not been copyedited and formatted. The final version may differ from this version.

Introduction

Compounds such as guanidines and aminopyridines that enhance neurotransmitter release have tremendous potential for treating neuromuscular diseases such as botulism, myasthenia gravis, the myasthenic syndrome of Lambert-Eaton, and multiple sclerosis (Wulff and Zhorov, 2008). Indeed, guanidine hydrochloride is sold as a prescription drug for the symptomatic treatment of Lambert-Eaton myasthenic syndrome (Keogh et al., 2011). Guanidine has also been used for the treatment of botulism (Chalk et al., 2011). Recently, the U.S. Food and Drug Administration approved 4-aminopyridine as a drug for the treatment of multiple sclerosis under the trade name Ampyra (Hauser and Johnston, 2010). Another aminopyridine compound, 3,4 diaminopyridine, is used in the treatment of botulism (Chalk et al., 2011; Mayorov et al., 2010) and Lambert-Eaton myasthenic syndrome (Keogh et al., 2011). A major limitation of the therapeutic use of these compounds is the harmful side effects that accompany their administration. Indeed, guanidine consumption can cause bone marrow suppression and renal failure (Blumhardt et al., 1977), and aminopyridines can penetrate the blood brain barrier and cause neurotoxicity (Mayorov et al., 2010). To overcome these detrimental side effects, it would be desirable to design analogs of aminopyridines and guanidines that exhibit high potency for their biological targets, enabling administration at low dosage levels.

Both aminopyridines and guanidine are known to stimulate neurotransmitter release by inhibiting presynaptic Kv channels (Benoit, 1993; Lundh and Thesleff, 1977). Aminopyridines inhibit Kv channels by binding to their pores (Armstrong and Loboda, 2001). Site-directed mutagenesis studies (Shieh and Kirsch, 1994; Zhang et al., 1998),

Molecular Pharmacology Fast Forward. Published on September 16, 2011 as DOI: 10.1124/mol.111.074989
This article has not been copyedited and formatted. The final version may differ from this version.

together with high resolution crystal structures of potassium channels, have provided valuable information on their binding site. This information has been judiciously utilized for rational drug design on the aminopyridine template. For example, docking simulations on the binding site (Caballero et al., 2007) have facilitated structure-activity studies on aminopyridines, leading to the generation of molecules with better therapeutic indices (Mayorov et al., 2010). In contrast, the mechanism of inhibition of Kv channels by guanidine has never been investigated thoroughly, and there are no published structure-activity studies on the guanidine scaffold. Indeed, no guanidine compound other than the underivatized guanidine molecule has been tested for treating any neuromuscular disorder.

The targets of aminopyridines and guanidines, Kv channels, are tetrameric ion channels, with each monomer consisting of six transmembrane segments (S1–S6). The S1–S4 domain functions as the voltage sensor and the S5–S6 region forms the pore (Fig. 1a). Extensive functional and structural studies have provided a detailed understanding of the mechanism of voltage sensing and gating in Kv channels. Voltage sensing is orchestrated by positively charged arginine residues of the S4 helix, which sense the electric field and drive motion of the voltage sensors (Aggarwal and MacKinnon, 1996; Seoh et al., 1996; Swartz, 2008). The surrounding membrane phospholipids interact intimately with the channel and play a vital role in voltage sensing (Jiang et al., 2003a; Jiang et al., 2003b; Ramu et al., 2006; Schmidt et al., 2006; Xu et al., 2008). The voltage sensors are linked to the pore by the S4–S5 linker, which couples voltage sensor motion to pore opening and closing (Long et al., 2005; Lu et al., 2001; Lu et al., 2002; Sukhareva et al., 2003). A Kv channel-inhibitor can, therefore, target several potential sites to inhibit

Molecular Pharmacology Fast Forward. Published on September 16, 2011 as DOI: 10.1124/mol.111.074989
This article has not been copyedited and formatted. The final version may differ from this version.

channel activity (Fig. 1a). For example, guanidine compounds might interact with the negatively charged phosphates of phospholipids displayed on the external surface of the membrane, resulting in a decrease in the surface potential, a phenomenon referred to as charge screening (Green and Andersen, 1991). A second potential site of action of guanidine compounds is the protein-lipid interface. One such interface might be formed by the positively charged arginine residues of the S4 helix, which face the outer leaflet of the membrane in the crystal structure of the open state of the channel (Long et al., 2007), suggesting that they may be involved in functionally significant arginine-phosphate interactions with the surrounding phospholipids that stabilize the activated state of the voltage sensor (Schmidt et al., 2006). Since guanidines are proficient at chelating the phosphate group, they might disrupt arginine-phospholipid interactions by sequestering the phosphate headgroups of phospholipids, resulting in inhibition. Another protein-lipid interface that is a potential target for guanidine compounds is the S4–S5 linker. This interface was revealed by the crystal structure of the Kv1.2-Kv2.1 chimera, which shows a lipid molecule bound to this region of the protein (Long et al., 2007). Finally, alkyl guanidines might inhibit Kv channels by binding to either the extracellular or the intracellular part of the pore of the channel, reminiscent of the action of peptides and organic cations such as the tetraethylammonium ion (TEA^+) and 4-aminopyridine ($4\text{-}AP^+$) (Wulff and Zhorov, 2008).

To investigate the aforementioned hypotheses, we performed a detailed investigation of the mechanism of inhibition of the Shaker potassium channel by guanidine (Gdn^+), methyl guanidine ($MeGdn^+$), and *N*,*N*-dimethyl guanidine ($DiMeGdn^+$)

Molecular Pharmacology Fast Forward. Published on September 16, 2011 as DOI: 10.1124/mol.111.074989
This article has not been copyedited and formatted. The final version may differ from this version.

(Fig. 1b). We find that these inhibitors bind within the intracellular pore of the channel, and perturb a hydrophobic subunit interface to stabilize a closed state of the channel.

Materials and Methods.

The pH of all buffer solutions was adjusted by adding NaOH. The Kv channel, Shaker H4, was utilized for the study. All constructs, including the one referred to as "wild-type", contained a deletion of residues 6-46 to remove fast inactivation (Hoshi et al., 1990). Site-directed mutagenesis, and channel expression in *Xenopus* oocytes were performed as described earlier (Sukhareva et al., 2003).

Two-electrode voltage-clamp recording from *Xenopus* oocytes. Currents were recorded using an OC-725C oocyte clamp (Warner Instruments). Data was filtered at 1 kHz (8-pole Bessel), and digitized at 10 kHz. Microelectrode resistances were between 0.1–1.2 MΩ when filled with 3M KCl. Inhibition was monitored by holding oocytes for an hour and pulsing to +10 mV every 10 sec while treating with guanidine compounds. Holding oocytes for an hour is technically challenging, and can result in leaching of KCl from the electrodes into oocytes, leading to a change in the intracellular concentration of K^+ ions. Due to this effect, the K^+ currents in control experiments are slightly larger after recording for 1h, and the inhibitory effects of guanidine compounds are underestimated. Solutions for recording and for overnight incubations and pretreatments of oocytes with guanidine compounds contained (in mM) RbCl (50), $MgCl_2$ (1), $CaCl_2$ (0.3), HEPES (20), and either Gdn.HCl (50), MeGdn.HCl (50), or $(DiMeGdn)_2SO_4$ (25), at pH 7.4. The corresponding control solutions contained NaCl instead of Gdn.HCl and MeGdn.HCl, and Na_2SO_4 instead of $(DiMeGdn)_2SO_4$. Whole cell ionic currents shown were obtained

Molecular Pharmacology Fast Forward. Published on September 16, 2011 as DOI: 10.1124/mol.111.074989
This article has not been copyedited and formatted. The final version may differ from this version.

by subtracting leak and background currents from whole cell currents by blocking the channel with the pore blocking toxin, Agitoxin-2 (Sukhareva et al., 2003), except for the R362Q, R365Q, R368Q triple mutant, which required high depolarizations for activation resulting in unbinding of the toxin, thereby preventing block.

Inside-out patch clamp recording. Guanidine compounds were applied intracellularly by pulling patches from oocytes expressing Shaker channels such that the intracellular part of the membrane was exposed to the recording chamber (the inside-out configuration). Currents were recorded using an Axopatch 200B patch clamp amplifier. The data was filtered at 2 kHz (8-pole Bessel), and digitized at 10 kHz. The batch solution was exchanged rapidly (~10-50 ms) using a computer-controlled perfusion system (RSC-200; Biologic). The bath solution contained (in mM) KCl (110), ethylene glycol tetraacetic acid (1), $MgCl_2$ (0.5), HEPES (10), and either Na_2SO_4 (25) or $(DiMeGdn)_2SO_4$ (25), at pH 7.4. The pipette solution contained (in mM) KCl (5), $MgCl_2$ (1), $CaCl_2$ (3), Na_2SO_4 (77.5), and HEPES (10) at pH 7.4. The resistance of the pipettes when filled with pipette solution was 0.5–2 MΩ.

Analysis of channel activity. Conductance (G)–Voltage (V) relationships were obtained by measuring steady state currents and using them to calculate the conductance. A single Boltzmann function was fitted to the data according to the equation, $G/G_{max} = [1+\exp(-zF(V-V_{1/2})/RT)]^{-1}$. To obtain Charge (Q)–Voltage (V) relationships from gating current experiments, Q values were obtained by integrating capacitive currents and subtracting values obtained from control oocytes from those measured in oocytes expressing high levels of W434F Shaker (~10^9 channels per oocyte) (Perozo et al., 1993). A single Boltzmann function was fitted to the data.

Molecular Pharmacology Fast Forward. Published on September 16, 2011 as DOI: 10.1124/mol.111.074989
This article has not been copyedited and formatted. The final version may differ from this version.

Oocyte uptake and washout assays with radiolabeled DiMeGdn$^+$. Tritiated $(DiMeGdn)_2SO_4$ (specific activity = 0.037 Ci/mmol) was purchased from Ambios Labs (Newington, CT), and dissolved to a concentration of 10 mM in a solution containing (in mM) HEPES (20), RbCl (50), $CaCl_2$ (0.3), $MgCl_2$ (1), and Na_2SO_4 (15) at pH 7.4 before storing at 4°C. Radioactivity measurements were performed on sets of 10 oocytes per scintillation vial.

Results.

To study the effect of guanidine compounds on Kv channels we employed the Shaker channel because it is a particularly well characterized Kv channel (Swartz, 2008; Yellen, 2002), and is therefore an ideal system for the mechanistic studies we sought to undertake.

Extracellular application of guanidines on oocytes expressing Shaker channels. Replacement of Na^+ in the external recording solution with 50 mM concentrations of Gdn^+, $MeGdn^+$, or $DiMeGdn^+$ resulted in slow inhibition of the Shaker channel (Fig. 2a,b). In addition to a reduction in the magnitude of depolarization-activated currents, the inhibition observed after 1 h is characterized by slowing of channel opening, and speeding of channel closure (Fig. 2a). The conductance (G)–voltage (V) plots are shifted rightwards after 1 h-treatment with guanidines (Fig. 2c, and Supplemental Table 1), suggesting that the inhibitors shift the closed-open equilibrium towards the closed state.

To determine the extent of steady-state inhibition, we incubated Shaker-expressing oocytes overnight with 50 mM Gdn^+, $MeGdn^+$ and $DiMeGdn^+$. $DiMeGdn^+$-treatment resulted in complete inhibition of Shaker (Fig. 3a). Indeed,

Molecular Pharmacology Fast Forward. Published on September 16, 2011 as DOI: 10.1124/mol.111.074989
This article has not been copyedited and formatted. The final version may differ from this version.

depolarizations as large as +160 mV failed to elicit any significant currents in $DiMeGdn^+$-treated oocytes (Fig. 3b). Interestingly, the results from both 1h and overnight treatment experiments demonstrate a direct correlation between the hydrophobicity of guanidine compounds, and the rate and extent of their inhibitory activities (Gdn^+<$MeGdn^+$<$DiMeGdn^+$).

Our data strongly suggests that the ability of these compounds to inhibit Kv channels is not due to extraneous effects such as their toxicity to oocytes. We found that despite extremely long incubations (>12 h) in 50 mM concentrations of these compounds, very few oocytes perished and appeared healthier than under control conditions. Furthermore, we faced no problems such as leakiness of oocytes while performing our two-electrode voltage-clamp experiments, consistent with the conclusion that these compounds were not toxic to oocytes. To further validate this conclusion, we tested the activity of another voltage-gated ion channel, TRPM8, after overnight incubation of oocytes expressing these channels with $DiMeGdn^+$. We found that $DiMeGdn^+$ had no detectable effects on TRPM8 currents (Supplemental Fig. 1), demonstrating that the effect of guanidine compounds on Kv channels is due to a specific action of these compounds.

Shaker channels inhibited by 1h-treatments with guanidine compounds did not recover despite thorough rinsing in control solutions, suggesting that recovery was too slow to observe under our continuous recording conditions (data not shown). To explore this phenomenon further, we treated uninjected oocytes with Gdn^+, $MeGdn^+$, or $DiMeGdn^+$ overnight, followed by removing guanidine compounds from the extracellular solution by thorough washing before injection of Shaker cRNA. These “pretreated”

Molecular Pharmacology Fast Forward. Published on September 16, 2011 as DOI: 10.1124/mol.111.074989
This article has not been copyedited and formatted. The final version may differ from this version.

oocytes were incubated in buffer solutions devoid of guanidine compounds for >12 h while the Shaker Kv channel was expressing prior to recording Kv channel currents. The results show that inhibition is profound, despite the absence of guanidine compounds in the external recording solution (Fig. 4). Kinetic analyses on pretreated oocytes expressing Shaker demonstrate that guanidines reduce the rate of channel opening (Supplemental Fig. 2). Indeed, depolarization of Shaker channels expressed in Na^+-pretreated oocytes to 0 mV results in channel opening with τ value of ~2 ms, which is lower than the τ values of channels expressed in Gdn^+-pretreated oocytes (~4 ms), $MeGdn^+$-pretreated oocytes (~5 ms) and $DiMeGdn^+$-pretreated oocytes (~8 ms). The kinetics of channel closure is also perturbed by the inhibitors—the channels close faster in the presence of the inhibitors (lower τ values at voltages between -80 and -40 mV in Supplemental Fig. 2).

These pretreatment experiments demonstrate the slow reversibility of inhibition of Shaker expressed in oocytes when guanidines are applied to the external solution. A comparison of the G–V plots (Fig. 4b and Fig. 3b) shows that the relative rates of recovery following removal of external guanidines occur in the following order: Gdn^+>$MeGdn^+$>$DiMeGdn^+$. Therefore, the inhibition of Shaker channels by extracellular application of $DiMeGdn^+$ is the most potent and the least reversible among the three guanidine compounds tested. Since the inhibitors do not actually need to be present in the extracellular solution to inhibit the channel, an extracellular pore-blocking mechanism of inhibition can be ruled out.

Interaction of radiolabeled $DiMeGdn^+$ with oocytes. The long-lived inhibition (slow recovery rate), as demonstrated by the pretreatment experiments, was surprising. Even if the inhibitors were acting intracellularly, they should be amenable to reversal within a

Molecular Pharmacology Fast Forward. Published on September 16, 2011 as DOI: 10.1124/mol.111.074989
This article has not been copyedited and formatted. The final version may differ from this version.

reasonable amount of time. For example, 4-AP^+ acts on Kv channels intracellularly, but channels recover within a minute following removal of the inhibitor from the external solution (del Camino et al., 2005). In contrast, inhibition of Shaker by guanidine reagents lasted >12 h after treatment (Fig. 4). Therefore, we decided to explore the interaction of $DiMeGdn^+$ with oocytes in more detail by measuring binding and unbinding of radiolabeled $DiMeGdn^+$ to oocytes. Our results (Supplemental Fig. 3a) show that the rate of uptake of $DiMeGdn^+$ in oocytes is very slow ($t_{1/2}$ = 19 h), and that $DiMeGdn^+$ has a high longevity in oocytes (Supplemental Fig. 3b). Indeed, even after incubating oocytes in wash buffer for 3 days, the amount of $DiMeGdn^+$ adhering to oocytes was reduced by only ~50%. The slow binding and unbinding kinetics observed for guanidines interacting with oocytes are similar to those observed for inhibition of the Shaker Kv channel, suggesting that interaction of these compounds with oocytes are responsible for the slow inhibition.

Does $DiMeGdn^+$ inhibit Shaker by disrupting the protein-lipid interface at the S4 helix? The long-lived binding of $DiMeGdn^+$ to oocytes and the results of the pretreatment experiment raise the possibility of a lipid-mediated mechanism of inhibition. Such a mechanism would be consistent with the order of potency of the guanidine molecules ($DiMeGdn^+$>$MeGdn^+$>Gdn^+), as an increase in hydrophobicity would allow for an increased ability to partition in the membrane, resulting in a higher extent of inhibition. For example, guanidine inhibitors may act by chelating to the phosphate head groups of phospholipids that are engaged in interactions with the outer three arginine residues of the S4 helix that carry gating charge (Aggarwal and MacKinnon, 1996; Seoh et al., 1996). These arginine-phosphate interactions are believed to stabilize the activated

Molecular Pharmacology Fast Forward. Published on September 16, 2011 as DOI: 10.1124/mol.111.074989
This article has not been copyedited and formatted. The final version may differ from this version.

state of the voltage sensors (Long et al., 2007; Ramu et al., 2006; Schmidt et al., 2006; Xu et al., 2008). If guanidines inhibit the channel by disrupting these interactions, we would expect that mutating the arginines to glutamines should disrupt the lipid interaction, producing a channel with activity reminiscent of what is observed in guanidines, and preventing further inhibition by these molecules. Although the triple mutant (R362Q, R365Q, R368Q) requires strong depolarization to activate, qualitatively resembling the effects of $DiMeGdn^+$ on the wild-type channel, it is profoundly inhibited by $DiMeGdn^+$ (Supplemental Fig. 4). These results suggest that $DiMeGdn^+$ does not inhibit the Shaker Kv channel by targeting this protein-lipid interface at the S4 helix.

Testing whether $DiMeGdn^+$ influences voltage sensor activation. To explore whether the inhibitory mechanism of guanidines involves interactions with the voltage sensors, we examined the effect of Gdn^+, $MeGdn^+$, and $DiMeGdn^+$ on the motion of the voltage sensors by measuring "gating currents". Gating currents occur as a component of the transient current following voltage steps and are produced as a result of the motion of the voltage sensors prior to channel opening (Perozo et al., 1993; Stefani et al., 1994). Non-conducting Shaker mutants such as W434F can be utilized to study gating currents without the obfuscating presence of ionic currents (Perozo et al., 1993). Fig. 5a shows the effects of $DiMeGdn^+$ on gating currents recorded from W434F-expressing oocytes after overnight treatment. The currents shown have two components—a linear capacitive component corresponding to charging of the membrane, and a non-linear component corresponding to the motion of the voltage sensors of Shaker. The depolarization-activated gating currents due to the motion of the voltage sensors from the resting to the activated state (the "on" gating currents) are not affected by $DiMeGdn^+$

Molecular Pharmacology Fast Forward. Published on September 16, 2011 as DOI: 10.1124/mol.111.074989
This article has not been copyedited and formatted. The final version may differ from this version.

(Fig. 5a). Similar results are obtained for Gdn^+ and $MeGdn^+$-treated oocytes (Supplemental Fig. 5). Indeed, the plot of the total amount of charge (Q) moved as a function of voltage (V) is indistinguishable when comparing untreated oocytes with those treated with each of the three guanidines (Fig. 5c). Therefore, these inhibitors have no obvious effects on the motion of the voltage sensors upon activation, and the amount of charge moved is the same in untreated and inhibitor-treated oocytes.

The only effect of guanidine compounds on gating currents is on the "off" gating currents, which are a manifestation of the return of the voltage sensors from the activated to the resting state upon hyperpolarization. It has been established that the voltage sensors of Kv channels are delayed in their motion from the activated to the resting state upon return from voltages where the gate opens (typically > -50 mV) (Batulan et al., 2010; Perozo et al., 1993; Stefani et al., 1994). This phenomenon is clearly observed in the off gating currents from control oocytes (Fig. 5a, top), however, after treatment with $DiMeGdn^+$ this delay is no longer apparent (Fig. 5a, bottom). Speeding of off gating currents was also observed for Gdn^+- and $MeGdn^+$-treated oocytes, and the extent of speeding correlated with the potency of inhibition of the compounds (Supplemental Fig. 5). In another version of this experiment, a W434F-expressing oocyte was treated with $DiMeGdn^+$ while recording gating currents (Fig. 5b). After 1h-treatment with $DiMeGdn^+$, there is a clear speeding of the off gating currents (the non-linear component of the curve in Fig. 5b) and negligible effects on the on gating currents (red trace in Fig. 5b).

The results from gating current measurements suggest that guanidines inhibit the Shaker Kv channel by influencing regions of the channel that are involved in the gating steps further downstream of the motion of the voltage sensor.

Molecular Pharmacology Fast Forward. Published on September 16, 2011 as DOI: 10.1124/mol.111.074989
This article has not been copyedited and formatted. The final version may differ from this version.

Among the three guanidine compounds, $DiMeGdn^+$ was the easiest to work with due to its relatively rapid kinetics and highest potency of inhibition (Fig. 2), and was therefore utilized for the rest of the experiments. The speeding of off gating currents by all three guanidine compounds tested (Fig. 5 and Supplemental Fig. 5), and qualitatively similar characteristics of inhibition (slowing down of channel opening and speeding of channel closure, as shown in Fig. 2–4 and Supplemental Fig. 2) suggest that the three compounds act by a similar mechanism. Therefore, it is reasonable to assume that the mechanistic insights obtained by utilizing $DiMeGdn^+$ would be valid for the other two compounds as well.

Does $DiMeGdn^+$ inhibit Kv channels by disrupting a protein-lipid interface at the S4–S5 linker? The S4–S5 linker is critical for coupling motions of the voltage sensors to opening of the intracellular gate (Batulan et al., 2010; Long et al., 2005; Lu et al., 2001; Lu et al., 2002). Interestingly, the crystal structure of the Kv1.2-Kv2.1 chimera shows a lipid molecule interacting with the S4–S5 linker (Supplemental Fig. 6a) and therefore guanidines may cause inhibition by disrupting this protein-lipid interface. Two residues in the S4–S5 linker, K380 and R387 (which is a Q in the crystal structure), are in close proximity to the phosphate group of the phospholipid molecule (Supplemental Fig. 6a). If guanidines inhibit the channel by disrupting these interactions, we would expect that replacing these charged residues with alanines should disrupt these lipid interactions, producing channels with activity similar to what is observed after guanidine-treatment of wild-type Shaker. Moreover, these mutated channels should be guanidine-insensitive. Our results show that both K380A and R387A display relatively wild-type gating

Molecular Pharmacology Fast Forward. Published on September 16, 2011 as DOI: 10.1124/mol.111.074989
This article has not been copyedited and formatted. The final version may differ from this version.

behavior, and were profoundly inhibited by $DiMeGdn^+$ (Supplemental Fig. 6b), suggesting that the inhibition is not mediated by this mechanism.

Mutation in the pore influence sensitivity to $DiMeGdn^+$. Our mutagenesis experiments on the voltage sensing machinery of the Shaker Kv channel described above strongly suggest that these regions of the channel are not targeted by guanidines. Therefore, we next focused on the pore region of the channel.

The P475 residue of the pore is located at a kink in the S6 helix (Fig. 6a), and could be responsible for creating it (Webster et al., 2004). This putative structural significance of P475 motivated us to start our studies on the pore at this position. We studied a P475 mutant whose gating properties were similar to those of the wild-type channel, P475F (Sukhareva et al., 2003), and found that it was not inhibited by 1h $DiMeGdn^+$-treatment (Fig. 6b).

The lack of inhibition by $DiMeGdn^+$ of a mutant that possesses gating characteristics similar to the wild-type channel suggests that the mutation disrupts binding of the inhibitor. Nevertheless, it is not clear whether the binding site is composed of the P475 residue, as mutation of a proline can cause significant structural changes in the S6 helix around the 475 position. For example, it is possible that mutation of the P475 residue results in the removal of the kink in the S6 helix, which disrupts the actual $DiMeGdn^+$ receptor further below or above the P475 residue.

The C-terminal end of the S6 helix has three aromatic amino acids (Y483, F484, and Y485; Supplemental Fig. 7a) that could interact with guanidines via cation-pi intertactions (Zacharias and Dougherty, 2002), and thus participate in forming the

Molecular Pharmacology Fast Forward. Published on September 16, 2011 as DOI: 10.1124/mol.111.074989
This article has not been copyedited and formatted. The final version may differ from this version.

DiMeGdn$^+$ receptor. This hypothesis is particularly enticing as recent work has shown that the interaction of Y485 with the S4–S5 linker of an adjacent subunit is the structural basis for the slowing of off gating currents (Batulan et al., 2010)—a process that was affected by guanidine compounds (Fig. 5 and Supplemental Fig. 5). However, the mutants Y483A, F484A, and Y485A were completely inhibited by 1h DiMeGdn$^+$ treatment (Supplemental Fig. 7b), suggesting that DiMeGdn$^+$ does not inhibit the channel by forming cation-pi interactions with the C-terminal end of the S6 helix. Alanine mutants of other residues below P475, such as I477, V478, S479, N480, H486, R487, and E488 also demonstrated wild-type sensitivity to DiMeGdn$^+$ (data not shown).

We next focused on the part of the S6 helix above the P475 residue (Fig. 7a). T469A was strongly inhibited by 1h DiMeGdn$^+$ treatment, similar to wild-type type Shaker (G–V plots of this mutant before and after treatment with DiMeGdn$^+$ are shown in green in Fig. 7a). In contrast, V467A, L468A, I470A, and V474A were less sensitive to inhibition by DiMeGdn$^+$ to varying degrees. There was much reduced effect of DiMeGdn$^+$ on the mutants L468A and V474A as compared to wild-type Shaker (Fig .7b). Indeed, the G–V plots for V474A (red curves in Fig. 7a) does not display any rightward shift (Supplemental Table 2), and L468A (cyan curves in Fig. 7a) demonstrates only a 8.5 mV rightward shift as compared to a 57.1 mV rightward shift by the wild-type channel (Supplemental Table 2) upon DiMeGdn$^+$-treatment. The G–V plots of V467A (black curves in Fig. 7a) and I470A (dark yellow curves in Fig. 7a) are shifted rightwards after DiMeGdn$^+$-treatment, but the extent of shift is much less than that for the wild-type channel (Fig. 2c, and Supplemental Table 2). It is important to note that all these mutants display relatively modest alterations in gating properties as compared to the wild-type

Molecular Pharmacology Fast Forward. Published on September 16, 2011 as DOI: 10.1124/mol.111.074989
This article has not been copyedited and formatted. The final version may differ from this version.

channel, suggesting that the reduction in inhibitor sensitivity results from a perturbation in the binding of the inhibitor. All these residues are located in the cavity of the pore, above the gate which is believed to be formed by residues below V474 (del Camino and Yellen, 2001; Liu et al., 1997).

Fig. 7c and 7d show the subunit interface of the pore region of the Kv1.2-Kv2.1 chimera. The residues V467 and L468 from one subunit, and I470 and V474 from an adjacent subunit are shown in red. T469 is shown is green and P475 in blue. The structure shows that L468 of one subunit is in close proximity to V474 of the adjacent subunit (3.69 Å apart). Moreover, V467 from one subunit is in close proximity to I470 of the adjacent subunit (3.70 Å apart). Therefore, it appears that altering this hydrophobic subunit interface in the cavity of the pore can dramatically decrease sensitivity to $DiMeGdn^+$. This notion is strengthened by the observation that the alanine mutant of the T469 residue, which is adjacent to the residues forming the hydrophobic subunit interface, but is not present within the interface (Fig. 7c,d), exhibits wild-type sensitivity to $DiMeGdn^+$.

Interaction of $DiMeGdn^+$ with the intracellular region of Kv channels. If $DiMeGdn^+$ inhibits the channel by binding inside the cavity of the pore, it would likely act from the intracellular side of the membrane as the selectivity filter of the channel would prevent access to the cavity from the extracellular side.

To study the effects of intracellular application of guanidines on Kv channels, we applied $DiMeGdn^+$ to membrane patches in the inside-out configuration and observed that the channel was strongly inhibited by $DiMeGdn^+$ (Fig. 8a,b). The current traces and

Molecular Pharmacology Fast Forward. Published on September 16, 2011 as DOI: 10.1124/mol.111.074989
This article has not been copyedited and formatted. The final version may differ from this version.

the G–V plots before and after treatment (Fig. 8a,b) resemble those obtained after overnight external application of $DiMeGdn^+$ (Fig. 3a,b, respectively). The onset of inhibition upon internal application of $DiMeGdn^+$ was very rapid when depolarizations were applied to open the channel (Fig. 8d, top). Indeed, onset of inhibition was faster than the kinetics of channel opening (Fig. 8d, top), but was not detected when $DiMeGdn^+$ was applied only in the closed state (not shown). In another version of the experiment in Fig. 8d, top, we applied $DiMeGdn^+$ first at -100 mV where all channels are closed, and then at -50 mV where a few channels are open (instead of 0 mV in Figure 8d where all channels are open), slowing down the rate of inhibition for open channels so that the rates of inhibition in the closed and open states could be compared (Supplemental Fig. 9). We find that the rate of inhibition in the open state is much faster than in closed state. Indeed, after application of the inhibitor in the closed state, a depolarization to -50 mV results in an initial current of almost the same magnitude as in the first depolarization which was applied in a solution devoid of the inhibitor, suggesting that the inhibition was negligible in the closed state. Application of the inhibitor in the open state, however, results in rapid inhibition. Based on this data, we conclude that the inhibitor accesses its binding site within the pore only after the gate opens.

The rapid inhibition observed upon internal application stands in stark contrast to the slow inhibition observed upon extracellular application, suggesting that the inhibitor acts from the intracellular side of the membrane. This conclusion is consistent with our mutagenesis studies, which implicate intracellular regions of the pore in the binding site of guanidines.

Molecular Pharmacology Fast Forward. Published on September 16, 2011 as DOI: 10.1124/mol.111.074989
This article has not been copyedited and formatted. The final version may differ from this version.

To determine whether $DiMeGdn^+$ can be trapped within the internal pore of Shaker, we employed the T449V mutant of Shaker (Lopez-Barneo et al., 1993) because this construct exhibits a much slower rate of inactivation, allowing us to measure unbinding during long depolarizations without substantial channel inactivation. We incubated a patch expressing Shaker in $DiMeGdn^+$ to completely inhibit the channels, then removed the inhibitor from the internal solution for 80 seconds while holding the patch at -100 mV before depolarizing to 0 mV to assess whether the channel remained inhibited (Fig. 8d, top). We observed that the inhibitor remains bound in the closed state, and unbinds only in the open state, as demonstrated by a slow increase in the current upon depolarization (denoted by an arrow in Fig. 8d, top). Therefore, it appears that $DiMeGdn^+$ is trapped within the pore of the channel, and is released when the gate opens upon depolarization. An analogous experiment with the well-studied Kv channel-blocker, TEA^+ (Fig. 8d, bottom), shows that in contrast to $DiMeGdn^+$, TEA^+ is not trapped inside the pore and must unbind before the channels can close (Armstrong and Loboda, 2001; Holmgren et al., 1997). Trapping of $DiMeGdn^+$ within the pore, when considered together with the effects of guanidines on G–V relations (Fig. 2–4), the kinetics of channel opening (Fig. 2a and Supplemental Fig. 2) and off gating current (Fig. 5 and Supplemental Fig. 5), suggest that the inhibitors bind within the internal pore and stabilize the closed state of the channel.

We also examined the concentration-dependence of inhibition of the Shaker Kv channel by $DiMeGdn^+$, and obtained an IC_{50} value of 0.6 mM (Fig. 8c). This high IC_{50} value demonstrates that $DiMeGdn^+$ is a relatively low-affinity inhibitor of Kv channels,

Molecular Pharmacology Fast Forward. Published on September 16, 2011 as DOI: 10.1124/mol.111.074989
This article has not been copyedited and formatted. The final version may differ from this version.

and explains the requirement of high dosage levels of guanidine for the treatment of Lambert-Eaton syndrome.

Discussion.

The inhibitory effect of guanidine compounds on Kv channels was first observed on the neuromuscular junction and on nerve terminals (Benoit, 1993; Lundh and Thesleff, 1977). Some of these early reports suggested an external charge screening mechanism of inhibition of Kv channels by guanidine (Benoit, 1993). This conclusion was contested by others who argued that the inhibition was intracellular (Farley et al., 1979). These experiments were performed on complex nerve-muscle preparations, predating a contemporary understanding of Kv channel structure and mechanism, and precluding the use of experimental approaches that proved indispensible for our mechanistic investigation. Our results show that pore mutations can significantly reduce sensitivity to the inhibitor (Fig. 7), and that the inhibitor can be trapped inside the cavity within the pore (Fig. 8d), establishing that inhibition is not mediated by a charge screening mechanism. Additionally, we rule out other potential mechanisms of inhibition such as direct interaction of the compounds with the voltage sensor machinery, disruption of two putative protein-lipid interfaces, and external pore-blocking.

When viewed collectively, the results presented here suggest that guanidines bind within the pore and inhibit the channel by stabilizing a closed state of the channel. Guanidines shift the G–V relations to depolarized voltages (Fig. 2–4), slow the kinetics of activation (Fig. 2 and Supplemental Fig. 2), and can be trapped within the pore (Fig. 8d). In addition, all three guanidine compounds tested accelerate off gating currents (Fig.

Molecular Pharmacology Fast Forward. Published on September 16, 2011 as DOI: 10.1124/mol.111.074989
This article has not been copyedited and formatted. The final version may differ from this version.

5 and Supplemental Fig. 5). Speeding of off gating currents was first observed for 4-AP^+, and was demonstrated to be a result of the stabilization of the activated-not open state of channel, immediately before the open state (Armstrong and Loboda, 2001; del Camino et al., 2005). Does this similarity between the mode of action of 4-AP^+ and guanidines imply a common binding site? A mutagenesis study (Zhang et al., 1998) on Kv1.4 concluded that the residue T529 (the equivalent residue in Shaker is T469) belongs to the binding site of 4-AP^+. In contrast, our experiments show that mutation of T469 in Shaker retains wild-type sensitivity to $DiMeGdn^+$ (Fig. 7). Another study (Shieh and Kirsch, 1994) found that L327 in the S5 helix of Kv2.1 (equivalent to L396 in Shaker) interacts directly with 4-AP^+. Our experiments show that the corresponding residue in Shaker (L396) and several other residues in S5 in the vicinity of L396, display wild-type sensitivity to $DiMeGdn^+$ when mutated to alanine (data not shown). Nevertheless, I405 of Kv2.1 is believed to be part of the 4-AP^+-binding site (Shieh and Kirsch, 1994), and mutation of the equivalent residue in Shaker (V474) dramatically alters sensitivity to $DiMeGdn^+$ (Fig. 7a,b). When considering that both inhibitors bind to the pore and stabilize the closed state, these mutagenesis results suggest that $DiMeGdn^+$ and 4-AP^+ bind to overlapping, but not identical sites in the pore of the channel. One interesting implication of the mechanisms for guanidines and 4-AP^+ is that their ability to stabilize the closed state of the channel make them attractive additives to crystallization trials in attempting to solve the structure of a Kv channel in a pre-open closed state.

What is the chemistry of interaction of guanidines with Kv channels? Guanidines interact favorably with acidic residues via salt-bridging, and with aromatic residues via cation-pi interactions (Zacharias and Dougherty, 2002). Nevertheless, mutagenesis of

Molecular Pharmacology Fast Forward. Published on September 16, 2011 as DOI: 10.1124/mol.111.074989
This article has not been copyedited and formatted. The final version may differ from this version.

none of the acidic or aromatic residues of Shaker reduced sensitivity to $DiMeGdn^+$, ruling out inhibition via these interactions. Instead, the mutagenesis of several hydrophobic S6 residues at the subunit interface (Fig. 7) reduced $DiMeGdn^+$-sensitivity, suggesting that the binding involves hydrophobic interactions between the alkyl groups of the inhibitor and the side chains of the residues at the interface. Additionally, the guanidine group may engage in hydrogen bonding-interactions with the backbone amide groups at its receptor site via its protonated nitrogen atoms. It is as if guanidine compounds act as molecular glue preventing an important structural change at the intersubunit interface before channel opening, thereby stabilizing the closed state and inhibiting the channel. Theoretical and structural studies will provide useful insights on the chemistry of binding of guanidines to the channel.

Our experiments in which uninjected oocytes were pretreated with guanidine compounds before injection of Shaker cRNA (Fig. 4) suggest that oocytes function as "guanidine sponges" that accumulate these compounds, and bind to the Shaker channel upon expression in the cell membrane. This conclusion is also supported by our experiments with radiolabeled $DiMeGdn^+$ (Supplemental Fig. 3), that demonstrate a high longevity in oocytes. Although the underlying mechanism of this phenomenon is unclear, one possible explanation is that polyphosphate compounds enriched in oocyte yolk (Kumble and Kornberg, 1995) sequester guanidines and when Shaker channels are expressed on the cell membranes, a dynamic equilibrium is established between the polyphosphate-guanidine complex in the cytoplasm and the guanidine-Shaker complex. An important implication of our work is the discovery of potential drug candidates for targeting neuromuscular diseases. Our results are likely to be relevant to human Kv

Molecular Pharmacology Fast Forward. Published on September 16, 2011 as DOI: 10.1124/mol.111.074989
This article has not been copyedited and formatted. The final version may differ from this version.

channels due to the high degree of sequence similarity of the S6 helices between Shaker and neuronal Kv1 and Kv3 channels expressed presynaptically in the neuromuscular junction (http://www.iuphar-db.org/index.jsp; Supplemental Fig. 8). Indeed, all four residues that are important for guanidine sensitivity of Shaker (V467, L468, I470, and V474) are also present in human Kv1.1, Kv1.2, Kv1.8, and Kv3.1. Another interesting implication of our work is that hydrophobic guanidines such as $MeGdn^+$ and $DiMeGdn^+$ have the potential to be more efficacious drugs for the treatment of neuromuscular diseases, as compared to Gdn^+—the only guanidine compound that has been used to treat neuromuscular diseases. Indeed, we find that $MeGdn^+$ and $DiMeGdn^+$ are more potent and faster inhibitors of Kv channels as compared to Gdn^+ (Fig. 2–4). Our results lay the foundations for a detailed investigation of $DiMeGdn^+$, $MeGdn^+$, and other hydrophobic guanidines as drug candidates for targeting neuromuscular diseases. Towards this goal, structure-activity relationship studies of guanidine analogs possessing a range of hydrophobicity indices are logical next steps.

Acknowledgments

We thank F. Bosmans, P. Miranda-Fernandez, M. Holmgren, A. M. Lopez, J. A. Mindell, M. D. Shoulders, and members of the Swartz laboratory for helpful discussions.

Molecular Pharmacology Fast Forward. Published on September 16, 2011 as DOI: 10.1124/mol.111.074989
This article has not been copyedited and formatted. The final version may differ from this version.

Author contributions

Conceived the project: Kalia

Performed research design: Kalia and Swartz

Conducted experiments: Kalia

Performed data analysis: Kalia

Wrote the manuscript: Kalia and Swartz

Molecular Pharmacology Fast Forward. Published on September 16, 2011 as DOI: 10.1124/mol.111.074989
This article has not been copyedited and formatted. The final version may differ from this version.

References

Aggarwal SK and MacKinnon R (1996) Contribution of the S4 segment to gating charge in the Shaker K^+ channel. *Neuron* **16**(6):1169-1177.

Armstrong CM and Loboda A (2001) A model for 4-aminopyridine action on K channels: Similarities to tetraethylammonium ion action. *Biophys J* **81**(2):895-904.

Batulan Z, Haddad GA and Blunck R (2010) An intersubunit interaction between S4-S5 linker and S6 is responsible for the slow off-gating component in Shaker K^+ channels. *J Biol Chem* **285**(18):14005-14019.

Benoit E (1993) Interactions of guanidine and a related compound with potassium channels in frog myelinated nerve fibre. *Receptors Channels* **1**(3):181-191.

Blumhardt LD, Joekes AM, Marshall J and Philalithis PE (1977) Guanidine treatment and impaired renal function in the Eaton-Lambert syndrome. *Br Med J* **1**(6066):946-947.

Caballero NA, Melendez FJ, Nino A and Munoz-Caro C (2007) Molecular docking study of the binding of aminopyridines within the K^+ channel. *J Mol Model* **13**(5):579-586.

Chalk C, Benstead TJ and Keezer M (2011) Medical treatment for botulism. *Cochrane Database Syst Rev* **3**:CD008123.

del Camino D, Kanevsky M and Yellen G (2005) Status of the intracellular gate in the activated-not-open state of Shaker K^+ channels. *J Gen Physiol* **126**(5):419-428.

del Camino D and Yellen G (2001) Tight steric closure at the intracellular activation gate of a voltage- gated K^+ channel. *Neuron* **32**(4):649-656.

Farley JM, Glavinovic MI, Watanabe S and Narahashi T (1979) Stimulation of transmitter release by guanidine derivatives. *Neuroscience* **4**(10):1511-1519.

Green WN and Andersen OS (1991) Surface charges and ion channel function. *Annu Rev Physiol* **53**:341-359.

Hauser SL and Johnston SC (2010) 4-aminopyridine: New life for an old drug. *Ann Neurol* **68**(1):A8-9.

Holmgren M, Smith PL and Yellen G (1997) Trapping of organic blockers by closing of voltage-dependent K^+ channels: Evidence for a trap door mechanism of activation gating. *J Gen Physiol* **109**(5):527-535.

Hoshi T, Zagotta WN and Aldrich RW (1990) Biophysical and molecular mechanisms of Shaker potassium channel inactivation. *Science* **250**(4980):533-538.

Jiang Y, Lee A, Chen J, Ruta V, Cadene M, Chait BT and MacKinnon R (2003a) X-ray structure of a voltage-dependent K^+ channel. *Nature* **423**(6935):33-41.

Jiang Y, Ruta V, Chen J, Lee A and MacKinnon R (2003b) The principle of gating charge movement in a voltage-dependent K^+ channel. *Nature* **423**(6935):42-48.

Keogh M, Sedehizadeh S and Maddison P (2011) Treatment for Lambert-Eaton myasthenic syndrome. *Cochrane Database Syst Rev* **2**:CD003279.

Kumble KD and Kornberg A (1995) Inorganic polyphosphate in mammalian cells and tissues. *J Bio Chem* **270**(11):5818-5822.

Liu Y, Holmgren M, Jurman ME and Yellen G (1997) Gated access to the pore of a voltage-dependent K^+ channel. *Neuron* **19**(1):175-184.

Long SB, Campbell EB and Mackinnon R (2005) Voltage sensor of Kv1.2: Structural basis of electromechanical coupling. *Science* **309**(5736):903-908.

Long SB, Tao X, Campbell EB and MacKinnon R (2007) Atomic structure of a voltage-dependent K^+ channel in a lipid membrane-like environment. *Nature* **450**(7168):376-382.

Lopez-Barneo J, Hoshi T, Heinemann SH and Aldrich RW (1993) Effects of external cations and mutations in the pore region on C-type inactivation of Shaker potassium channels. *Receptors Channels* **1**(1):61-71.

Lu Z, Klem AM and Ramu Y (2001) Ion conduction pore is conserved among potassium channels. *Nature* **413**(6858):809-813.

Lu Z, Klem AM and Ramu Y (2002) Coupling between voltage sensors and activation gate in voltage-gated K^+ channels. *J Gen Physiol* **120**(5):663-676.

Lundh H and Thesleff S (1977) The mode of action of 4-aminopyridine and guanidine on transmitter release from motor nerve terminals. *Eur J Pharmacol* **42**(4):411-412.

Mayorov AV, Willis B, Di Mola A, Adler D, Borgia J, Jackson O, Wang J, Luo Y, Tang L, Knapp RJ, Natarajan C, Goodnough MC, Zilberberg N, Simpson LL and Janda KD (2010) Symptomatic relief of botulinum neurotoxin/a intoxication with aminopyridines: A new twist on an old molecule. *ACS Chem Biol* **5**(12):1183-1191.

Perozo E, MacKinnon R, Bezanilla F and Stefani E (1993) Gating currents from a nonconducting mutant reveal open-closed conformations in Shaker K+ channels. *Neuron* **11**(2):353-358.

Ramu Y, Xu Y and Lu Z (2006) Enzymatic activation of voltage-gated potassium channels. *Nature* **442**(7103):696-699.

Schmidt D, Jiang QX and MacKinnon R (2006) Phospholipids and the origin of cationic gating charges in voltage sensors. *Nature* **444**(7120):775-779.

Seoh SA, Sigg D, Papazian DM and Bezanilla F (1996) Voltage-sensing residues in the S2 and S4 segments of the Shaker K^+ channel. *Neuron* **16**(6):1159-1167.

Shieh CC and Kirsch GE (1994) Mutational analysis of ion conduction and drug binding sites in the inner mouth of voltage-gated K^+ channels. *Biophys J* **67**(6):2316-2325.

Stefani E, Toro L, Perozo E and Bezanilla F (1994) Gating of Shaker K^+ channels: I. Ionic and gating currents. *Biophys J* **66**(4):996-1010.

Sukhareva M, Hackos DH and Swartz KJ (2003) Constitutive activation of the Shaker Kv channel. *J Gen Physiol* **122**(5):541-556.

Swartz KJ (2008) Sensing voltage across lipid membranes. *Nature* **456**(7224):891-897.

Webster SM, Del Camino D, Dekker JP and Yellen G (2004) Intracellular gate opening in Shaker K^+ channels defined by high-affinity metal bridges. *Nature* **428**(6985):864-868.

Wulff H and Zhorov BS (2008) K^+ channel modulators for the treatment of neurological disorders and autoimmune diseases. *Chem Rev* **108**(5):1744-1773.

Xu Y, Ramu Y and Lu Z (2008) Removal of phospho-head groups of membrane lipids immobilizes voltage sensors of K^+ channels. *Nature* **451**(7180):826-829.

Yellen G (2002) The voltage-gated potassium channels and their relatives. *Nature* **419**(6902):35-42.

Zacharias N and Dougherty DA (2002) Cation-pi interactions in ligand recognition and catalysis. *Trends Pharmacol Sci* **23**(6):281-287.

Zhang H, Zhu B, Yao JA and Tseng GN (1998) Differential effects of S6 mutations on binding of quinidine and 4-aminopyridine to rat isoform of Kv1.4: common site but different factors in determining blockers' binding affinity. *J Pharmacol Exp Ther* **287**(1):332-343.

Molecular Pharmacology Fast Forward. Published on September 16, 2011 as DOI: 10.1124/mol.111.074989
This article has not been copyedited and formatted. The final version may differ from this version.

Footnotes

This work was supported by the Intramural Research Program of the NINDS, NIH to K. J. Swartz, and by the NINDS competitive fellowship to J. Kalia. Reprint requests can be sent to either J. Kalia (kaliaj@ninds.nih.gov) or K. J. Swartz (swartzk@ninds.nih.gov) at the following address: Porter Neuroscience Research Center, Molecular Physiology and Biophysics Section, National Institute of Neurological Disorders and Stroke, National Institutes of Health, 35 Convent Drive, Bethesda, Maryland 20892, USA.

Molecular Pharmacology Fast Forward. Published on September 16, 2011 as DOI: 10.1124/mol.111.074989
This article has not been copyedited and formatted. The final version may differ from this version.

Legends for figures

Figure 1. Inhibition of Kv channels by guanidine compounds. (**a**) Model illustrating the possible modes of inhibition of Kv channels by guanidine compounds (shown in red): screening of external negative charges on the membrane, disruption of protein-lipid interfaces at different sites, and binding to the extracellular or intracellular region of the channel pore Kv channels are tetramers containing four S1–S4 voltage-sensing domains, but only one is shown here for clarity. The central pore domain is formed by the S5–S6 helices from the four subunits. (**b**) The chemical structures of guanidine compounds used in this study.

Figure 2. Inhibition of Shaker Kv channel by guanidine compounds. (**a**) Families of ionic currents for wild-type Shaker channels before (left panel) and after (right panel) treatment with 50 mM Na^+, Gdn^+, $MeGdn^+$, or $DiMeGdn^+$. The holding voltage was -80 mV, tail voltage was -50 mV and depolarizations were from -80 mV to +90 mV in 10 mV increments. (**b**) Time course of inhibition of Shaker by Gdn^+, $MeGdn^+$, and $DiMeGdn^+$. Oocytes were held at -80 mV, and depolarized to +10 mV every 10 seconds while perfusing 50 mM guanidine compound for 1h. Guanidine treatment was started after a 3 min treatment with control solution. (**c**) G–V relations for the Shaker channel before and after 1h-treatment of oocytes. Error bars indicate s.e.m. (n = 3).

Figure 3. Overnight treatment of Shaker Kv channel with guanidine compounds. (**a**) Families of ionic currents for wild-type Shaker channels from oocytes treated overnight with 50 mM Na^+, Gdn^+, $MeGdn^+$, or $DiMeGdn^+$. The holding voltage was -80 mV, tail voltage was -50 mV and depolarizations were from -80 to +90 mV for Na^+ and Gdn^+

Molecular Pharmacology Fast Forward. Published on September 16, 2011 as DOI: 10.1124/mol.111.074989
This article has not been copyedited and formatted. The final version may differ from this version.

treated oocytes, and from -80 mV to +110 mV for $MeGdn^+$ and $DiMeGdn^+$ treated oocytes, in 10 mV increments. (**b**) G–V relations for the Shaker channel after overnight treatments Error bars indicate s.e.m. (n = 5).

Figure 4. Pretreatment of oocytes with guanidine compounds inhibit subsequently expressed Shaker Kv channels. (**a**) Families of ionic currents for wild-type Shaker channels from oocytes treated overnight with 50 mM Na^+, Gdn^+, $MeGdn^+$, and $DiMeGdn^+$ and then rinsed thoroughly to remove guanidines from the extracellular solution. After rinsing, oocytes were injected with Shaker cRNA, and currents were recorded in normal recording solution a day later. The holding voltage was -80 mV, tail voltage was -50 mV and depolarizations were from -80 mV to +100 mV in 10 mV increments. (**b**) G–V relations for the Shaker channel after pretreatment. Error bars indicate s.e.m. (n = 3).

Figure 5. Effect of guanidine compounds on movement of the Shaker voltage sensors. (**a**) Oocytes expressing the W434F Shaker mutant were either treated overnight with 50 mM $DiMeGdn^+$ (bottom), or incubated in a control solution (top) and then gating currents were elicited by holding the oocytes at -100 mV, and depolarizing in 5 mV increments from -100 mV to +20 mV. Off gating currents were obtained by subsequently hyperpolarizing to -100 mV. (**b**) An oocyte expressing the W434F mutant was held at -100 mV and depolarized to -25 mV and then hyperpolarized to -100 mV every 10 seconds with concomitant treatment with $DiMeGdn^+$ for 1h to monitor the effect of $DiMeGdn^+$ on the gating currents. The curve in black represents gating currents obtained before $DiMeGdn^+$ treatment, and the one in red represents gating currents after treatment. (**c**) Boltzmann equation fitted to a plot of gating charge (Q) and voltage (V) Q was

obtained from gating currents from W434F-injected oocytes treated with Gdn^+ (red symbols), $MeGdn^+$ (green symbols), $DiMeGdn^+$ (pink symbols) or control solutions (black circles). Error bars indicate s.e.m. (n = 3).

Figure 6. Mutating P475 renders the Shaker channel insensitive to inhibition by $DiMeGdn^+$. (**a**) Top: Sequence of the S6 helix of Shaker with P475 in red. Bottom: Ribbon representation of the pore region of the Kv1.2-Kv2.1 paddle chimera (PDB accession code 2R9R) showing P475 in red. (**b**) Families of ionic currents for the P475F mutant expressed in oocytes before (left panel) and after 1h-treatment (right panel) with 50 mM $DiMeGdn^+$. The holding voltage was -80 mV, tail voltage was -120 mV and depolarizations were from -80 mV to +90 mV in 10 mV increments. G–V relations for the P475F mutant before (filled symbols) and after 1h-treatment (empty symbols) with $DiMeGdn^+$ are shown at the bottom. Error bars indicate s.e.m. (n = 3).

Figure 7. Mutations in the S6 helix above P475 reduce sensitivity of Shaker to $DiMeGdn^+$. (**a**) Top: Sequence of the S6 helix of Shaker with the mutated residues under consideration in red. Bottom: G–V relations of the mutants before (filled symbols) and after 1 h-treatment with 50 mM $DiMeGdn^+$ (open symbols). Error bars indicate s.e.m. (n = 3). (**b**) Families of ionic currents for the mutants L468A and V474A before and after 1h-treatment with 50 mM $DiMeGdn^+$. The holding voltage was -80 mV, tail voltage was -80 mV and depolarizations were from -50 mV to +30 mV in 10 mV increments for L468A and from -80 mV to +60 mV in 10 mV increments for V474A. (**c**) View of the subunit interface of the pore showing the residues that reduce sensitivity to $DiMeGdn^+$ in red, T469 in green, and P475 in blue. (**d**) View of the subunit interface from the

Molecular Pharmacology Fast Forward. Published on September 16, 2011 as DOI: 10.1124/mol.111.074989
This article has not been copyedited and formatted. The final version may differ from this version.

extracellular side of the membrane. A turn of the helix formed by residues A463-A465 was removed from the structure to improve clarity.

Figure 8. Intracellular application of $DiMeGdn^+$ to inside-out oocyte patches expressing Shaker. (**a**) Families of ionic currents for wild-type Shaker before (left panel) and after (right panel) treatment with 50 mM $DiMeGdn^+$. The holding and tail voltages were -100 mV, and depolarizations were from -100 mV to -10 mV in 10 mV increments. Error bars indicate s.e.m. (n = 3). (**b**) G–V relations for Shaker before (left panel) and after (right panel) treatment with 50 mM $DiMeGdn^+$. (**c**) Dose response for inhibition of Shaker by $DiMeGdn^+$ fitted to a single binding site model, plotted as fraction unbound (Fu) measured at 0 mV (Error bars indicate s.e.m.; $n \geq 3$ for each point in the plot). (**d**) A patch expressing Shaker T449V was held at -100 mV and depolarized to 0 mV, first in buffer devoid of $DiMeGdn^+$, and then in the presence of $DiMeGdn^+$. The patch was then transferred back to a solution devoid of $DiMeGdn^+$ and incubated at -100 mV for 80 seconds before depolarizing to 0 mV. A similar experiment with TEA^+ is shown in the bottom panel**.**

Figure 1.

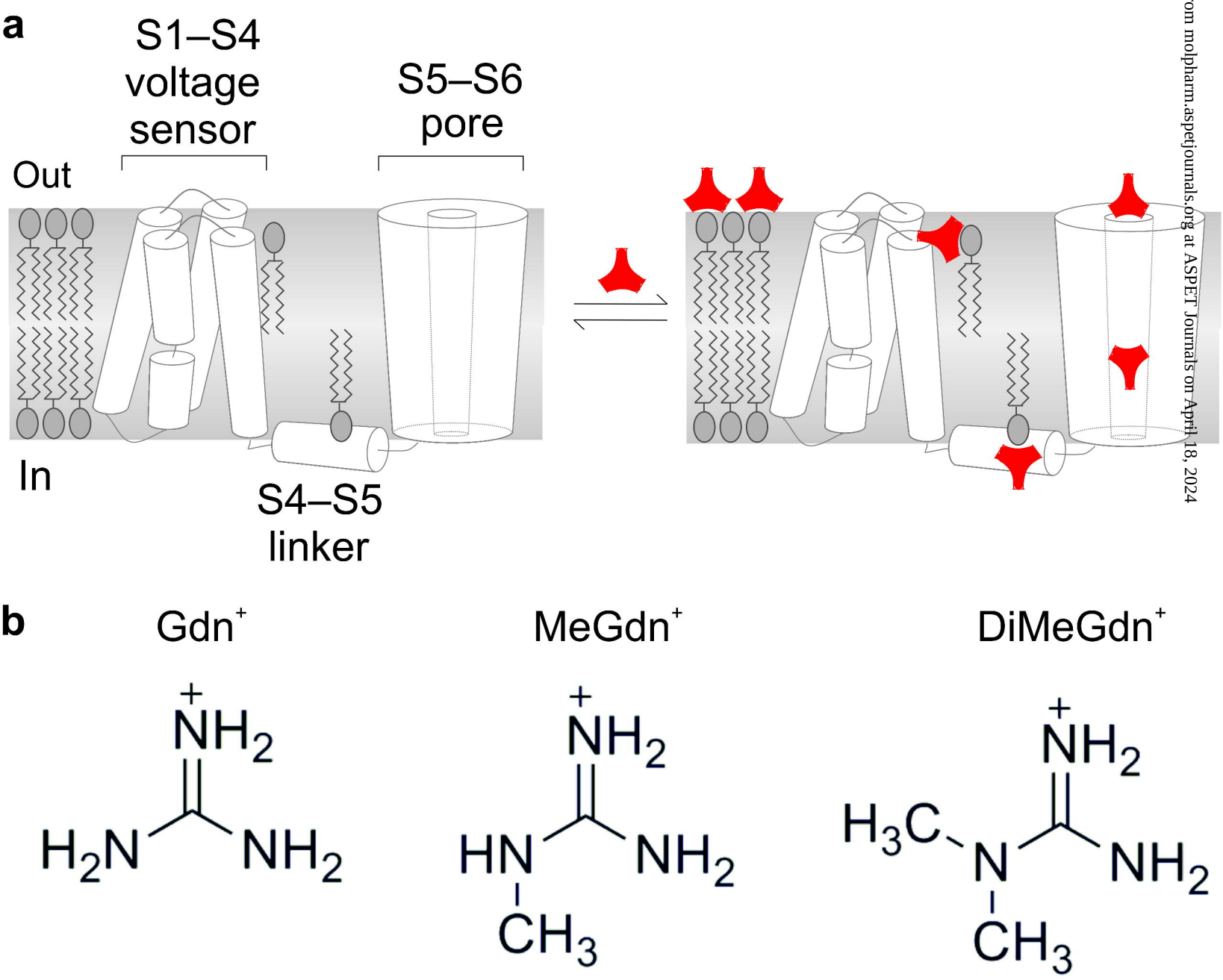

Figure 2.

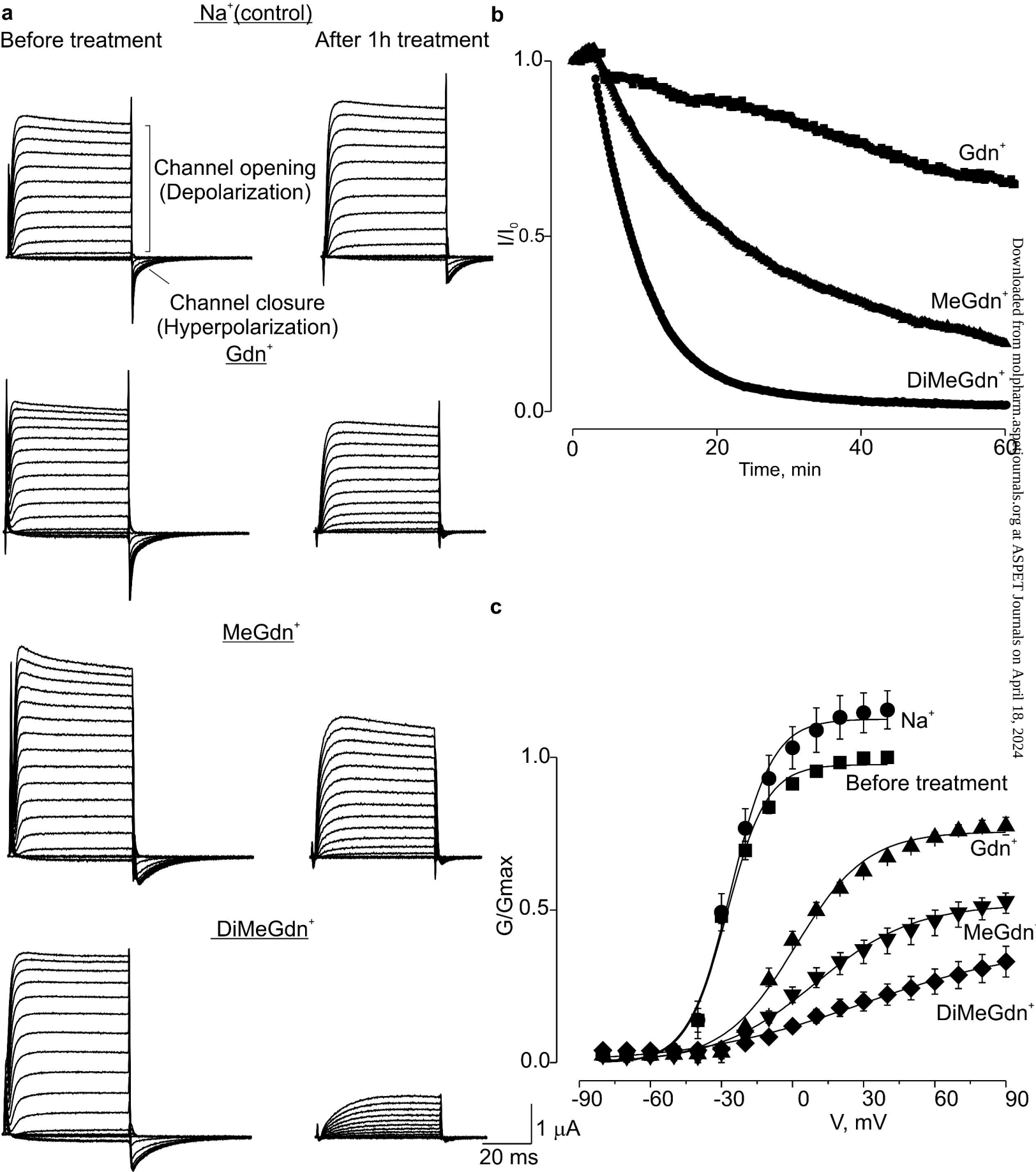

Figure 3.

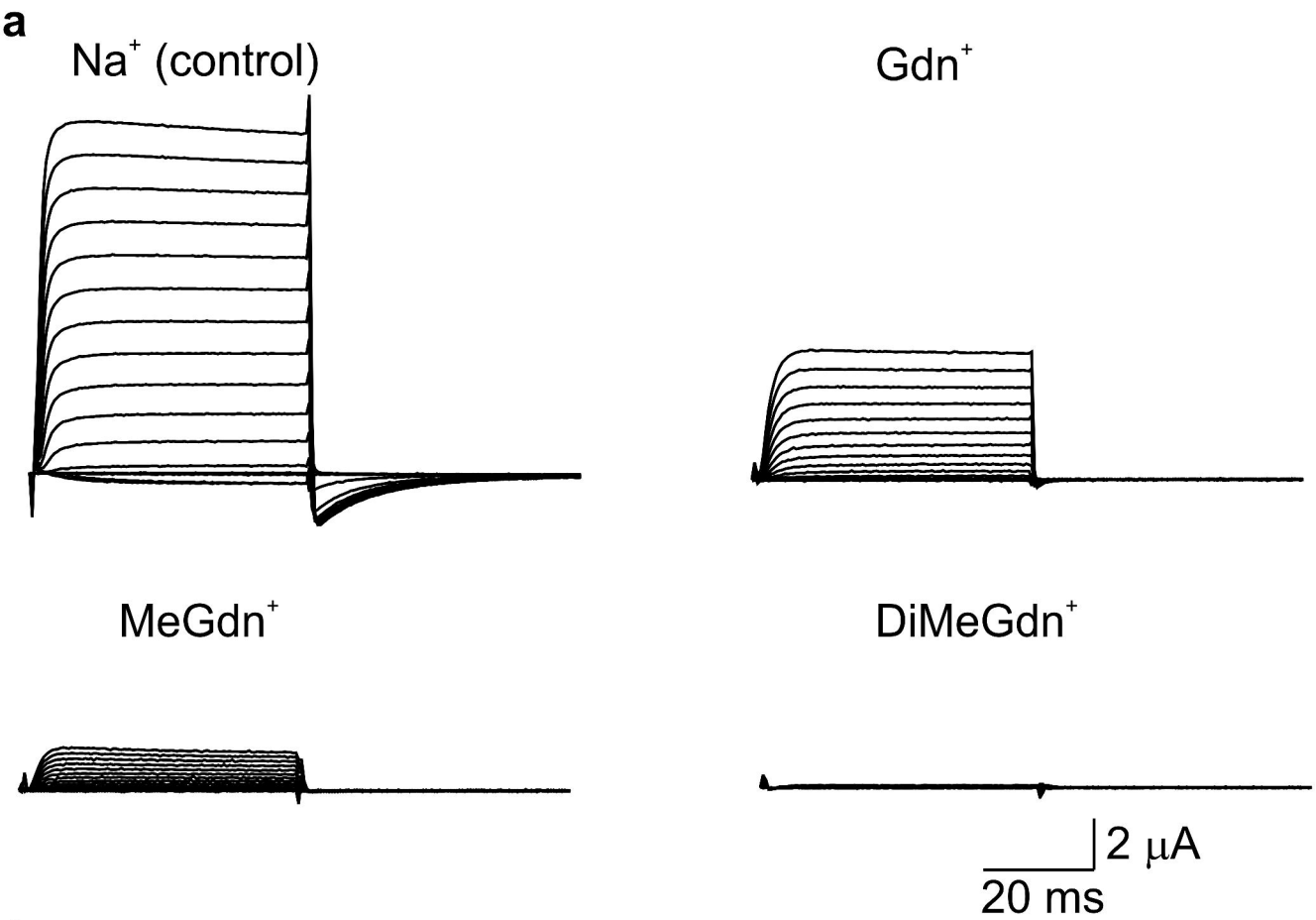
a
Na+ (control)
Gdn+
MeGdn+
DiMeGdn+
2 μA
20 ms

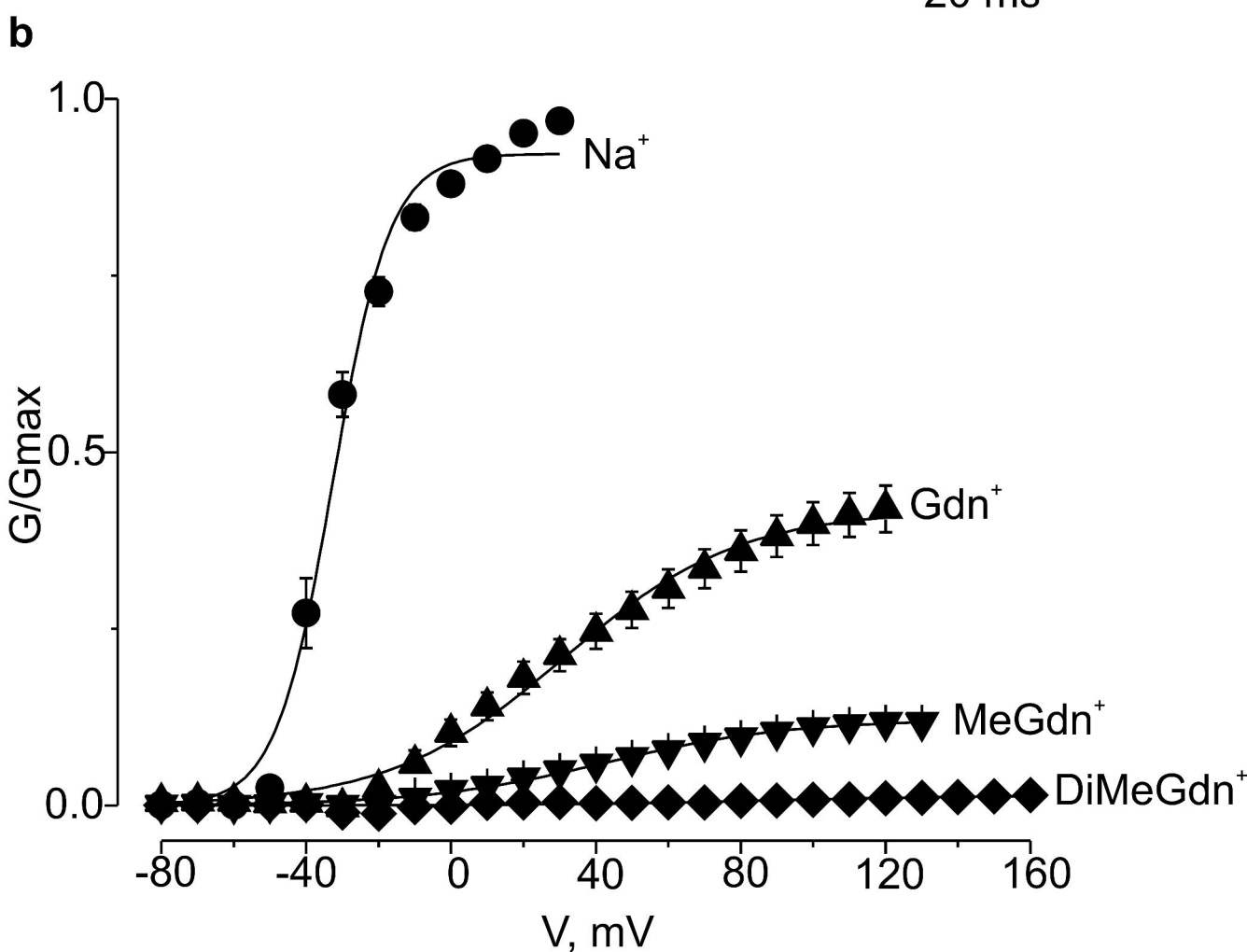
b
1.0
0.5
0.0
G/Gmax
Na+
Gdn+
MeGdn+
DiMeGdn+
-80
-40
0
40
80
120
160
V, mV

Figure 4.

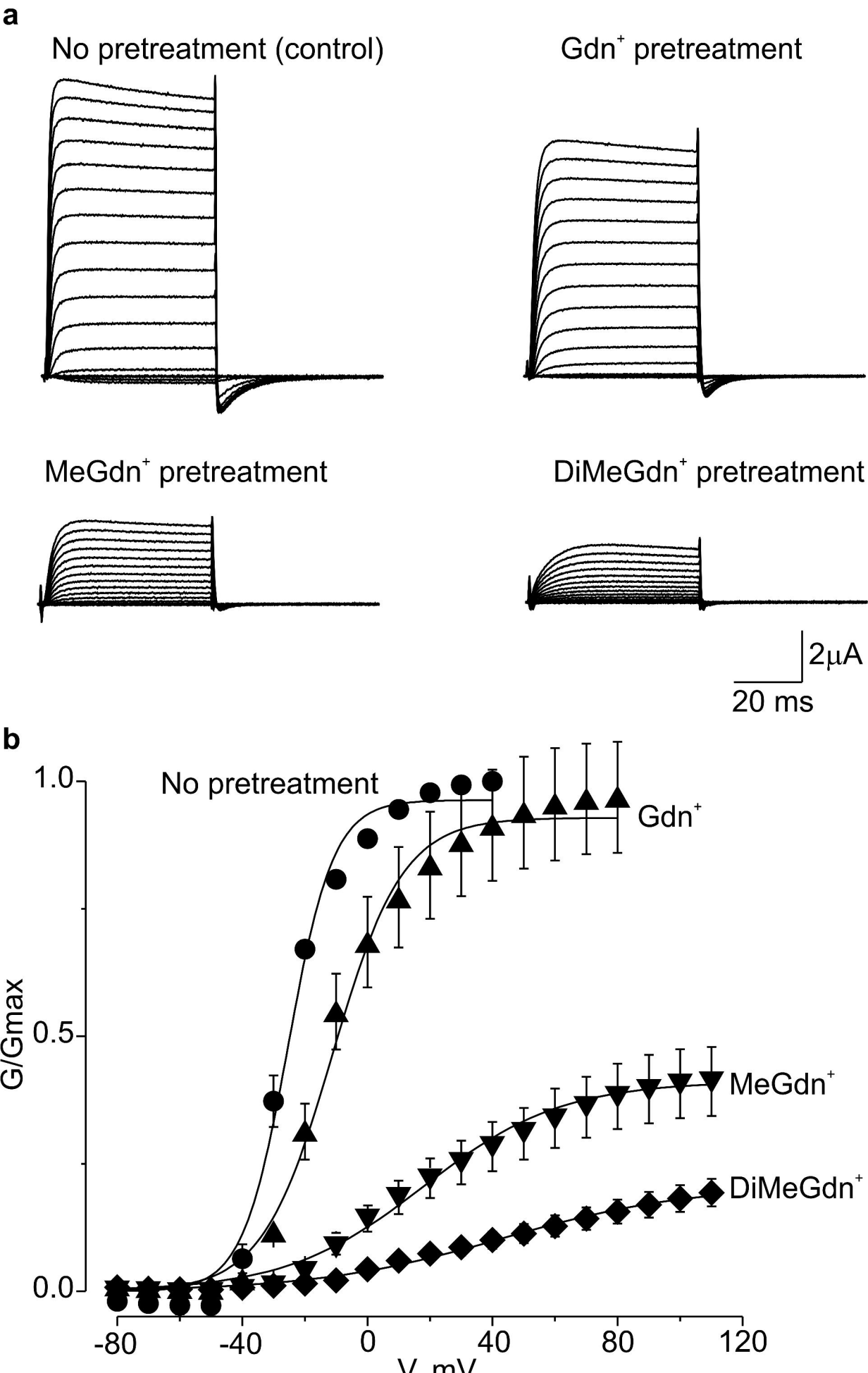
a
No pretreatment (control)
Gdn+ pretreatment
MeGdn+ pretreatment
DiMeGdn+ pretreatment
2μA
20 ms
b
No pretreatment
Gdn+
MeGdn+
DiMeGdn+
G/Gmax
1.0
0.5
0.0
-80
-40
0
40
80
120
V, mV

Figure 5.

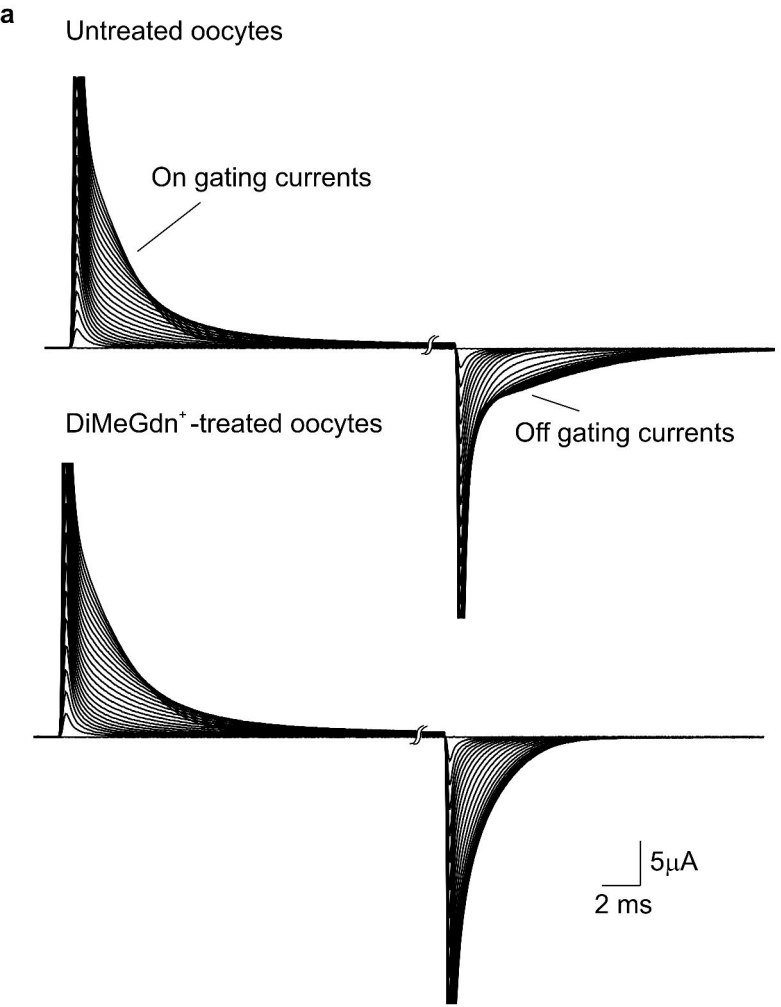

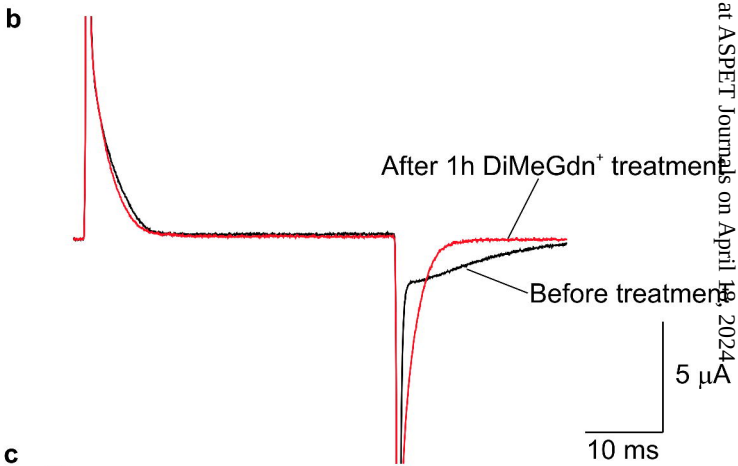

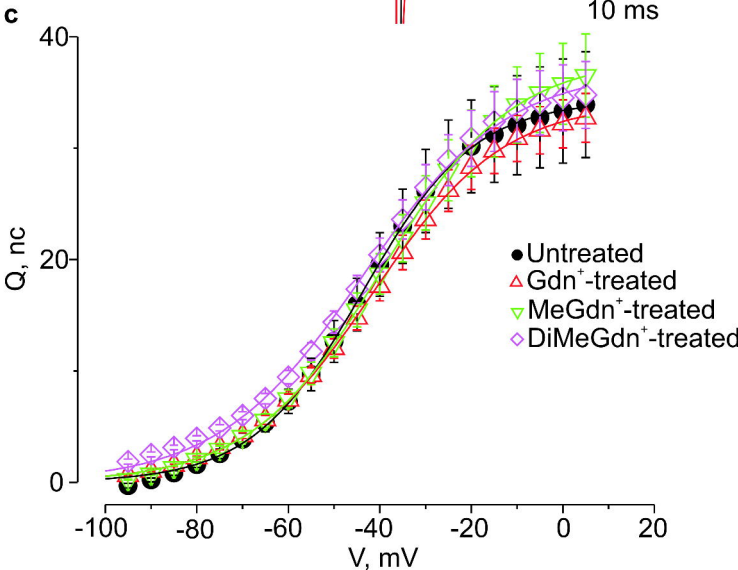

Figure 6.

a

S6 (452) GVWGKIVGSLCAIAGVLTIALPVPVIVSNFNYFYHRET (489)

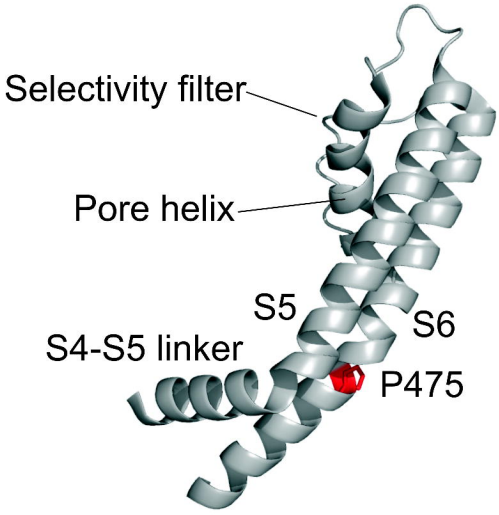

b

P475F

Before treatment

After 1h DiMeGdn^{+} treatment

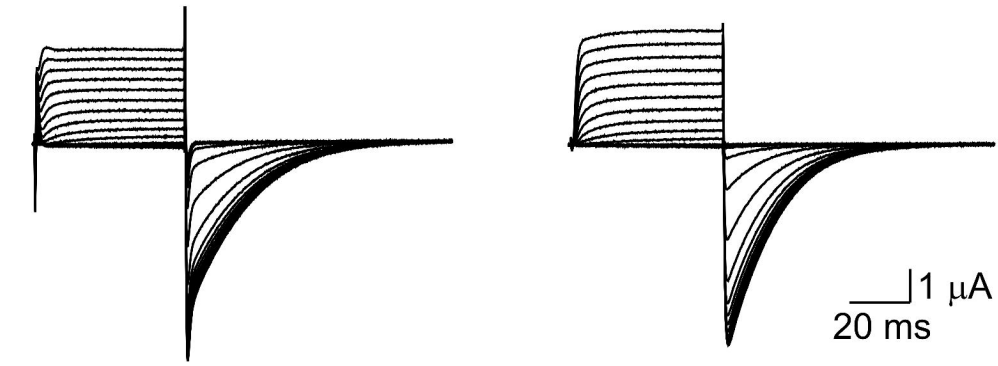

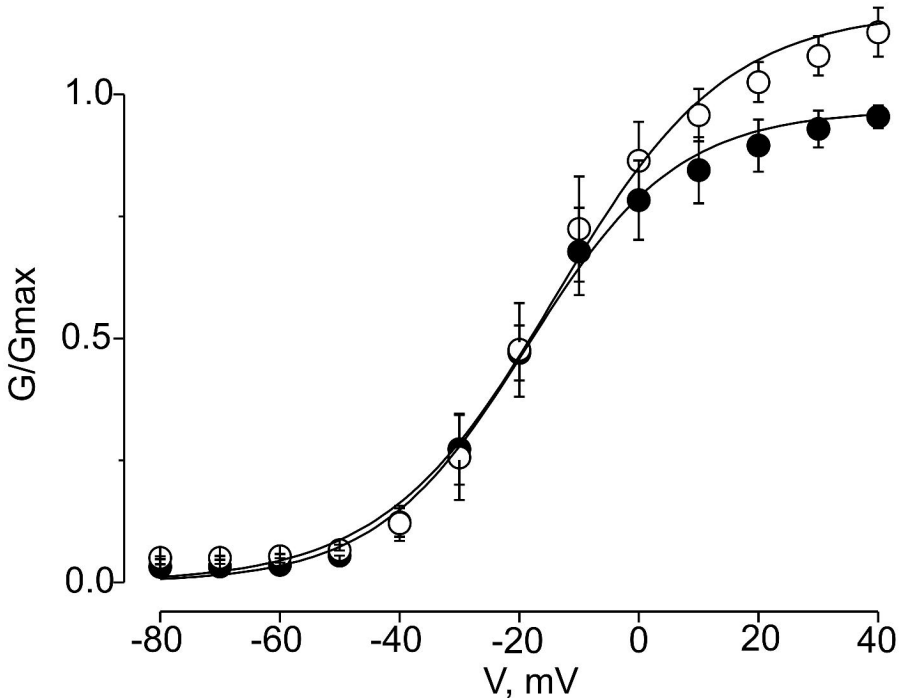

Figure 7.

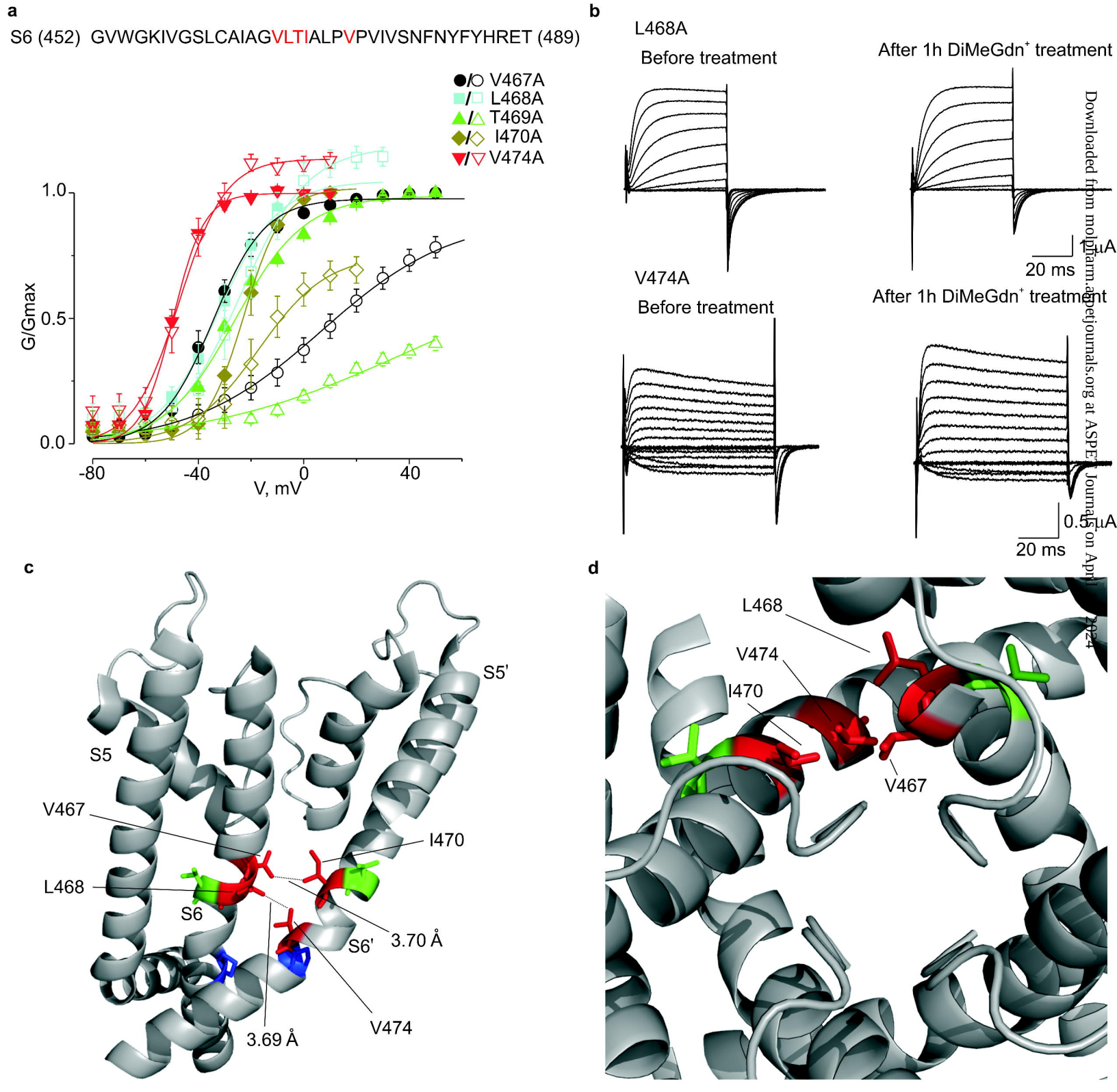

Figure 8.

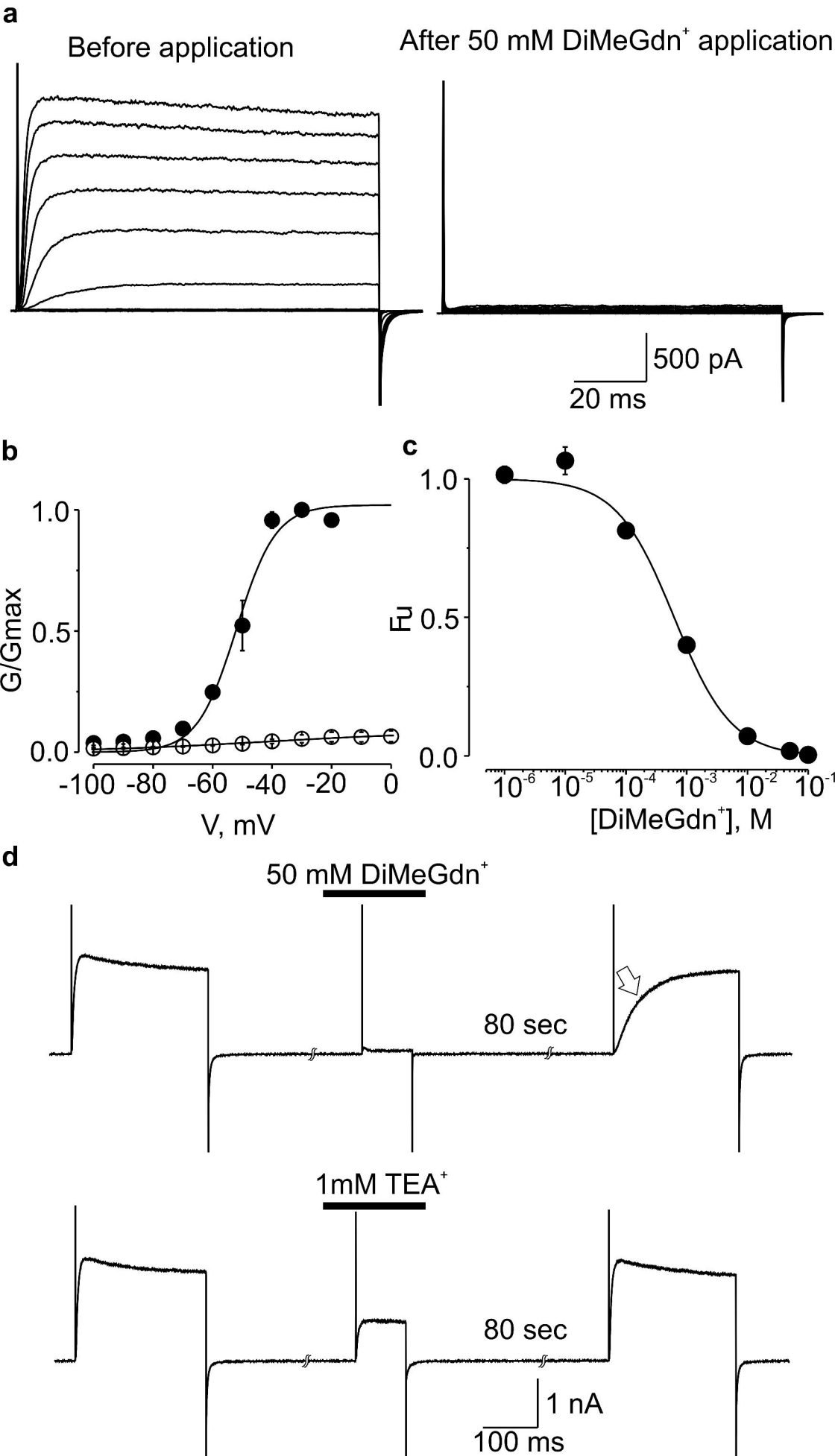
a
Before application
After 50 mM DiMeGdn+ application
500 pA
20 ms
b
1.0
0.5
0.0
G/Gmax
-100 -80 -60 -40 -20 0
V, mV
c
1.0
0.5
0.0
FU
10-6 10-5 10-4 10-3 10-2 10-1
[DiMeGdn+], M
d
50 mM DiMeGdn+
80 sec
1mM TEA+
80 sec
1 nA
100 ms

SUPPLEMENTAL DATA

Journal Title: Molecular Pharmacology

Elucidating the molecular basis of action of a classical drug: Guanidine compounds as inhibitors of voltage-gated potassium channels

Jeet Kalia and Kenton J. Swartz

Porter Neuroscience Research Center,

Molecular Physiology and Biophysics Section,

National Institute of Neurological Disorders and Stroke,

National Institutes of Health

35 Convent Drive,

Bethesda, Maryland 20892, USA

Address correspondence to:

Jeet Kalia (kaliaj@ninds.nih.gov) or Kenton Swartz (swartzk@ninds.nih.gov)

Telephone: (301) 435-5652; Fax: (301) 435-5666

Supplemental Figure 1

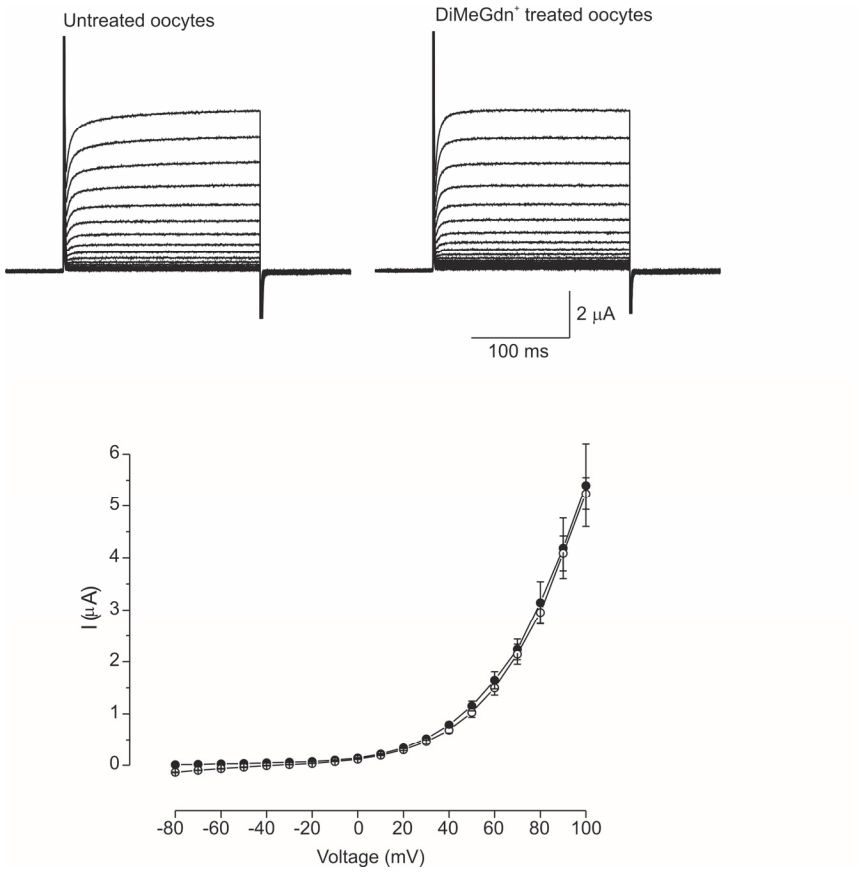

DiMeGdn$^+$ does not inhibit rat TRPM8. Top: Families of ionic currents for rat TRPM8 channels from oocytes treated overnight with 50 mM Na^+ or DiMeGdn$^+$. The holding voltage and tail voltage was -60 mV and depolarizations were from -80 to +100 mV in 10 mV increments. Bottom: I-V relations after overnight treatments with Na^+ (filled circles) and DiMeGdn$^+$ (open circles). The recording solution contained (in mM) HEPES (20), KCl (50), NaCl (50), $MgCl_2$ (1), and $BaCl_2$ (0.3) at pH 7.4.

Supplemental Figure 2

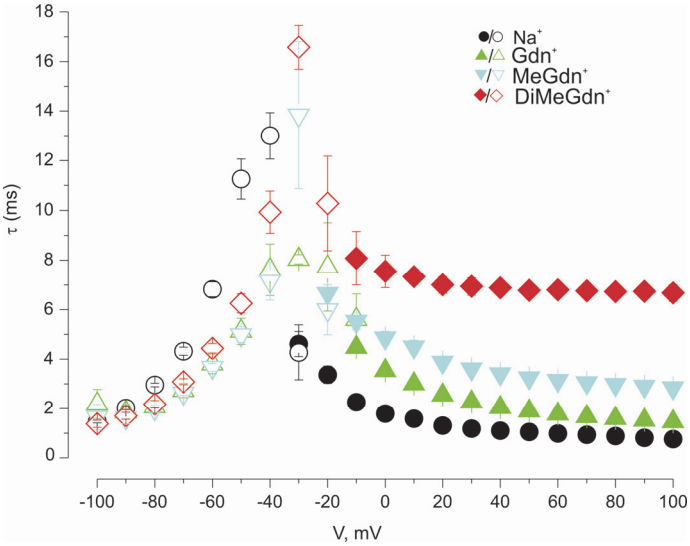

Effect of guanidine compounds on the kinetics of activation and deactivation of the Shaker channel. Oocytes pretreated with guanidine compounds were injected with Shaker cRNA and macroscopic currents corresponding to channel activation and deactivation were elicited a day after injection using the following protocols: activation, 10 mV incrementing steps to voltages between -30 to +100 mV (holding potential was -80 mV); deactivation, 10 mV incrementing steps to voltages between -20 and -100 mV after depolarizing to +100 mV (holding potential was -80 mV). Mean time constants (τ) from single exponential fits to channel activation (filled symbols) and deactivation (open symbols) were plotted as a function of the voltage at which currents were recorded. Error bars indicate s.e.m. (n = 3-5).

Supplemental Figure 3

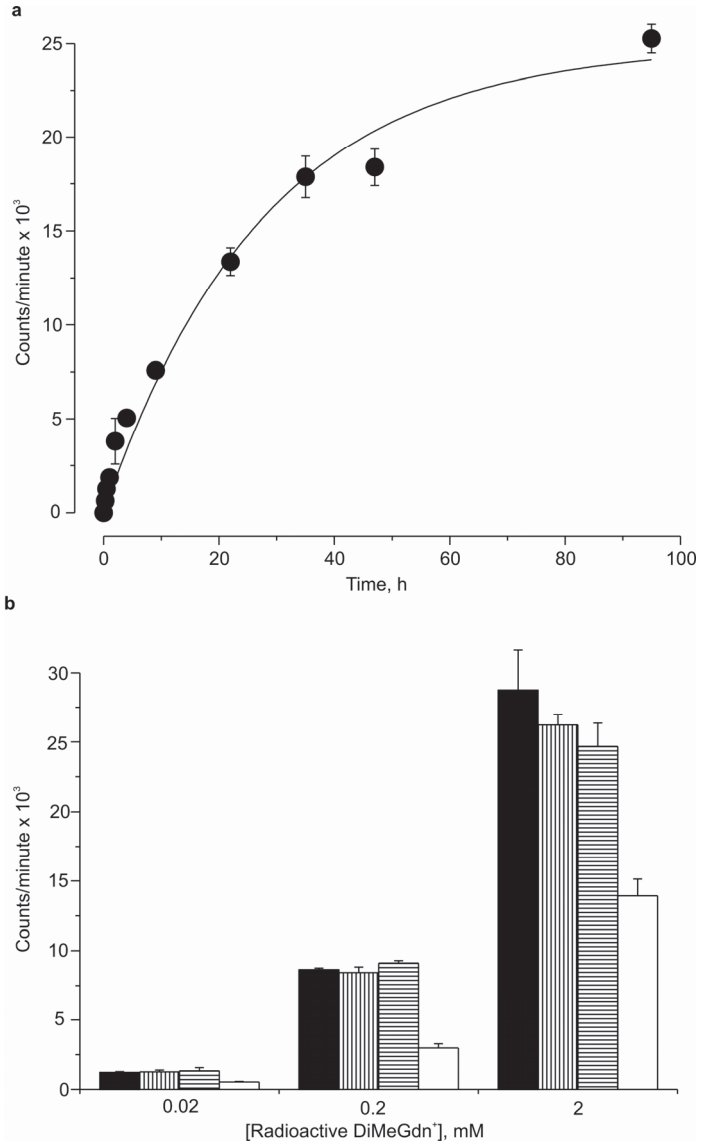

Interaction of radiolabeled DiMeGdn$^+$ with oocytes. (**a**). Oocytes were incubated in 20 mM radiolabeled DiMeGdn$^+$ and after different time intervals, 30 oocytes were isolated, rinsed thoroughly, and transferred to scintillation vials (10 oocytes in each via, n = 3) containing scintillation liquid and the radioactivity was measured to quantify uptake. A single exponential equation was fitted to a plot of counts per minute and time. (**b**) Oocytes were incubated in different concentrations of radiolabeled DiMeGdn$^+$ overnight, and the radioactivity was measured (in sets of 10 oocytes, n = 3) without rinsing (black bars), after rinsing with 50 mL buffer (bars with vertical lines), after two consecutive 50 mL-rinses (bars with horizontal lines), and after extensive rinsing by incubating in 10 mL wash buffer for 3 days followed by two consecutive 50 mL-rinses (white bars). Error bars indicate s.e.m. (n = 3).

Supplemental Figure 4

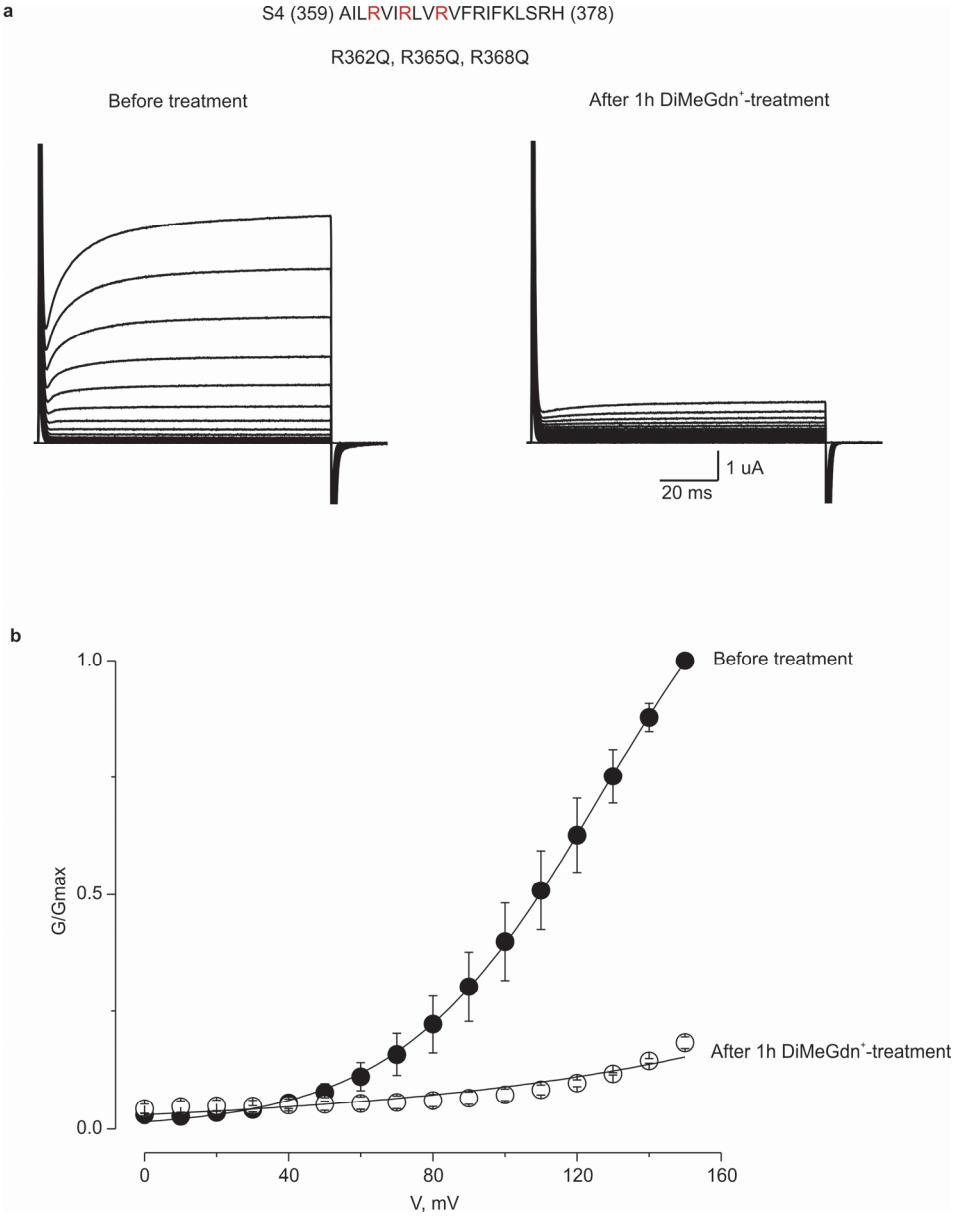

S4 arginine triple mutant of Shaker is inhibited by DiMeGdn$^+$. (**a**) Top: The sequence of the S4 helix of the Shaker channel with R362, R365, and R368 shown in red. Bottom: Families of ionic current records for the R362Q, R368Q, R371Q triple mutant. The record on the left is before DiMeGdn$^+$-treatment, and the one on the right is after 1h-treatment with DiMeGdn$^+$. The holding voltage was -20 mV, tail voltage was -20 mV and depolarizations were from -20 to +150 mV, in 10 mV increments. (**b**) G–V relations for the R362Q, R368Q, R371Q triple mutant channel before (filled circles) and after (open circles) 1h-treatment of oocytes with DiMeGdn$^+$. Error bars indicate s.e.m. (n = 3).

Supplemental Figure 5

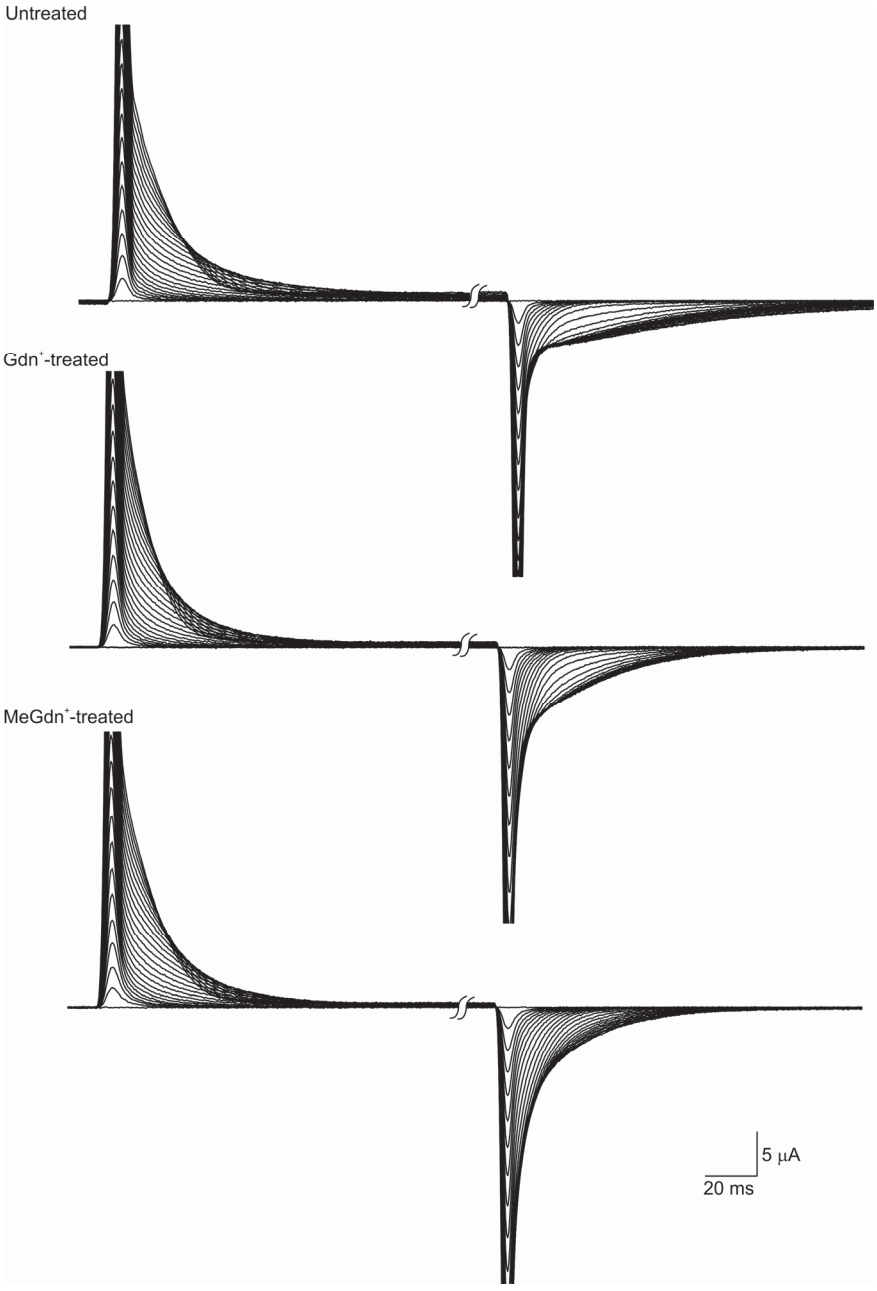

Effect of Gdn^+ and $MeGdn^+$ on the movement of the Shaker voltage sensors. Oocytes expressing the W434F Shaker mutant were either treated with 50 mM Gdn^+ (middle panel), 50 mM Me Gdn^+ (bottom panel), or incubated in a control solution (top panel) and then gating currents were elicited by holding the oocytes at -100 mV, and depolarizing in 5 mV increments from -100 mV to +20 mV. Off gating currents were obtained by subsequently hyperpolarizing to -100 mV.

Supplemental Figure 6

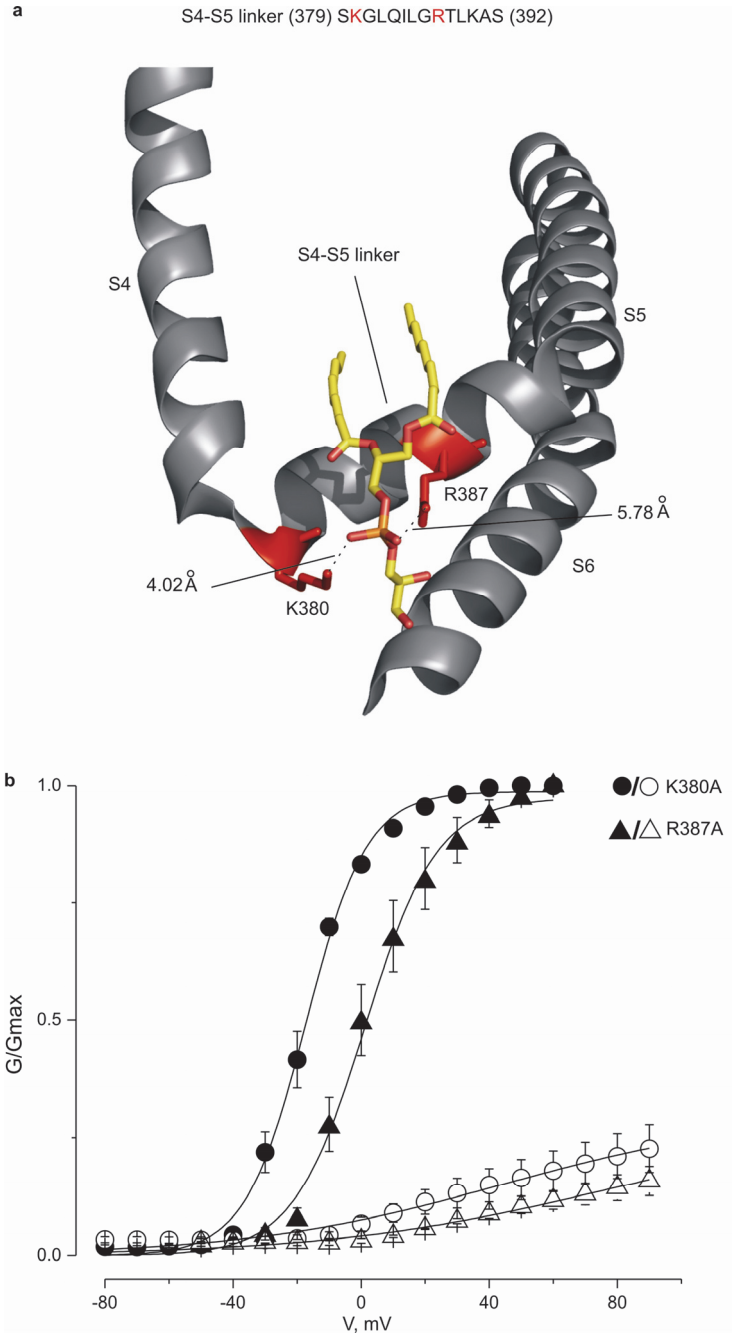

S4–S5 mutants of Shaker are inhibited by DiMeGdn^{+}. (**a**) Top: Sequence of the S4-S5 linker with K380 and R387 shown in red. Bottom: Ribbon representation of the S4-S5 linker region of the Kv1.2-Kv2.1 paddle chimera (PDB accession code 2R9R) with a lipid molecule bound (CPK representation, colored according to atom type: yellow, carbon; red, oxygen; magenta, phosphorus) (**b**) G–V relations for the K380A and R387A mutants before (filled symbols) and after (open symbols) 1h-treatment with DiMeGdn^{+}. For K380A, the holding voltage was -80 mV, tail voltage was -50 mV and depolarizations were from -80 to +60 mV, in 10 mV increments. For R387A, the holding voltage was -50 mV, tail voltage was -50 mV and depolarizations were from -50 to +60 mV, in 10 mV increments. Error bars indicate s.e.m. (n = 3).

Supplemental Figure 7

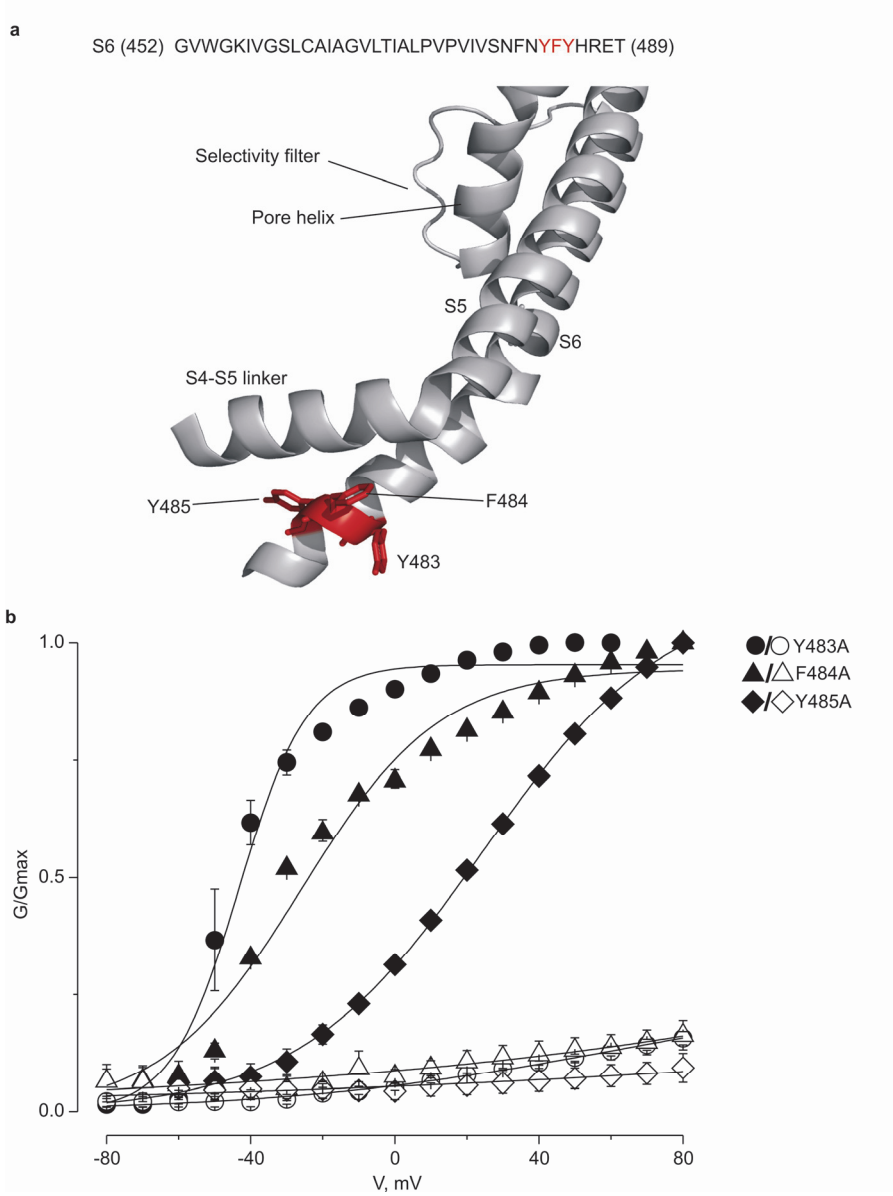

DiMeGdn$^+$ does not inhibit Shaker by forming cation-pi interactions with the S6 helix. (**a**) Top: Sequence of the S6 helix of Shaker with the aromatic residues in red. Bottom: Ribbon representation of the pore region of the Kv1.2-Kv2.1 paddle chimera (PDB accession code 2R9R) showing aromatic residues in red. (**b**) G–V relations for the alanine mutants of the aromatic residues in the S6 helix before (filled symbols) and after 1h-treatment (empty symbols) with 50 mM DiMeGdn$^+$. For Y483A, the holding voltage was -90 mV, tail voltage was -90 mV and depolarizations were from -90 to +80 mV, in 10 mV increments. For F484A, the holding voltage was -80 mV, tail voltage was -80 mV and depolarizations were from -80 to +80 mV, in 10 mV increments. For Y485A, the holding voltage was -80 mV, tail voltage was -80 mV and depolarizations were from -80 to +80 mV, in 10 mV increments. Error bars indicate s.e.m. (n = 3).

Supplemental Figure 8

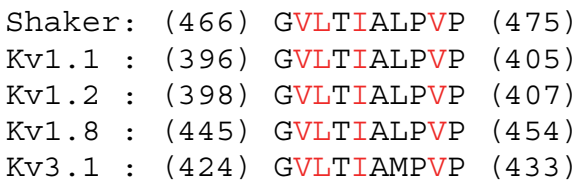

Sequence alignment of the portion of the Shaker S6 helix that is important for guanidine sensitivity with analogous regions of human Kv channels expressed presynaptically in neuromuscular junctions. The Shaker residues shown in red represent are important for guanidine-sensitivity. Corresponding residues in human Kv channels are also shown in red.

Supplemental Figure 9

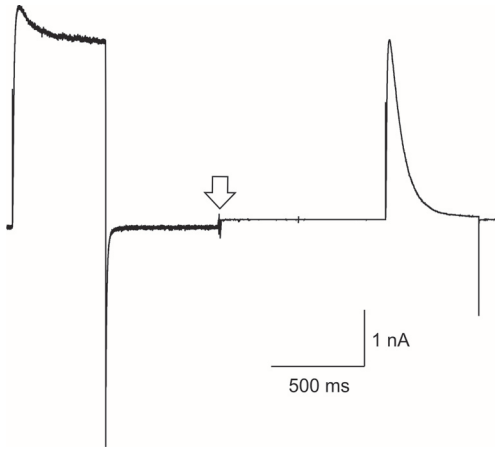

DiMeGdn$^+$ binds to Shaker preferably in the open state. An inside-out patch excised from an oocyte expressing Shaker was held at -100 mV and depolarized to -50 mV, first in buffer devoid of DiMeGdn$^+$, and then in buffer containing 50 mM DiMeGdn$^+$. The arrow denotes the point of transfer from the buffer devoid of DiMeGdn$^+$ to the one containing DiMeGdn$^+$.

Supplemental Table 1

Manuscript figure depicting corresponding G-V plot	Description of procedure of treatment with inhibitor	Boltzmann best-fit parameters	
		$V_{1/2}$	z
Figure 2b	Untreated	-27.8 ± 1.0	3.0 ± 0.3
Figure 2b	Na^+ (1h)	-26.1 ± 1.0	2.9 ± 0.3
Figure 2b	Gdn^+ (1h)	1.2 ± 0.1	1.7 ± 0.7
Figure 2b	$MeGdn^+$ (1h)	9.5 ± 2.0	1.2 ± 0.2
Figure 2b	$DiMeGdn^+$ (1h)	29.3 ± 6.0	0.7 ± 0.1
Figure 3b	Na^+ (overnight)	-31.5 ± 1.4	3.0 ± 0.4
Figure 3b	Gdn^+ (overnight)	31.2 ± 2.3	1.1 ± 0.1
Figure 3b	$MeGdn^+$ (overnight)	41.6 ± 2.6	1.0 ± 0.1
Figure 3b	$DiMeGdn^+$ (overnight)	ND	ND
Figure 4b	Na^+ (pretreatment)	-25.3 ± 1.2	3.5 ± 0.5
Figure 4b	Gdn^+ (pretreatment)	-11.2 ± 1.1	2.3 ± 0.2
Figure 4b	$MeGdn^+$ (pretreatment)	18.0 ± 2.2	1.2 ± 0.1
Figure 4b	$DiMeGdn^+$ (pretreatment)	43.0 ± 3.5	0.9 ± 0.1

Boltzmann best-fit parameters of wild-type Shaker channels after treatment with guanidine compounds. The values for experiments entailing overnight $DiMeGdn^+$-treatment could not be obtained because the channels were completely inhibited in these conditions, thereby precluding reliable measurements of best-fit parameters.

Supplemental Table 2

Shaker channel construct	Manuscript figure depicting corresponding G-V plot	Boltzmann best-fit parameters before treatment		Boltzmann best-fit parameters after treatment		$\Delta V_{1/2}$
		$V_{1/2}$	z	$V_{1/2}$	z	
wild-type	Figure 2b	-27.8 ± 1.0	3.0 ± 0.3	29.3 ± 6.0	0.7 ± 0.1	57.1
V467A	Figure 7a	-34.5 ± 0.9	2.6 ± 0.2	7.0 ± 1.6	1.0 ± 0.1	41.5
L468A	Figure 7a	-32.4 ± 1.0	2.2 ± 0.2	-23.9 ± 1.9	2.0 ± 0.3	8.5
T469A	Figure 7a	-26.0 ± 1.7	1.9 ± 0.2	37.7 ± 6.0	0.7 ± 0.4	63.7
I470A	Figure 7a	-22.7 ± 1.0	3.5 ± 0.4	-17.0 ± 3.6	2.0 ± 0.5	5.7
V474A	Figure 7a	-46.3 ± 4.6	2.6 ± 1.0	-47.2 ± 2.0	2.9 ± 0.6	-0.9

Boltzmann best-fit parameters of wild-type Shaker and S6 mutants of Shaker before and after 1h DiMeGdn$^+$ treatment.